

Weak boson emission in hadron collider processes

U. Baur*

Department of Physics, State University of New York, Buffalo, New York 14260, USA

(Received 17 November 2006; published 11 January 2007)

The $\mathcal{O}(\alpha)$ virtual weak radiative corrections to many hadron collider processes are known to become large and negative at high energies, due to the appearance of Sudakov-like logarithms. At the same order in perturbation theory, weak boson emission diagrams contribute. Since the W and Z bosons are massive, the $\mathcal{O}(\alpha)$ virtual weak radiative corrections and the contributions from weak boson emission are separately finite. Thus, unlike in QED or QCD calculations, there is no technical reason for including gauge boson emission diagrams in calculations of electroweak radiative corrections. In most calculations of the $\mathcal{O}(\alpha)$ electroweak radiative corrections, weak boson emission diagrams are therefore not taken into account. Another reason for not including these diagrams is that they lead to final states which differ from that of the original process. However, in experiment, one usually considers partially inclusive final states. Weak boson emission diagrams thus should be included in calculations of electroweak radiative corrections. In this paper, I examine the role of weak boson emission in those processes at the Fermilab Tevatron and the CERN LHC for which the one-loop electroweak radiative corrections are known to become large at high energies (inclusive jet, isolated photon, $Z + 1$ jet, Drell-Yan, di-boson, $\bar{t}t$, and single top production). In general, I find that the cross section for weak boson emission is substantial at high energies and that weak boson emission and the $\mathcal{O}(\alpha)$ virtual weak radiative corrections partially cancel.

DOI: [10.1103/PhysRevD.75.013005](https://doi.org/10.1103/PhysRevD.75.013005)

PACS numbers: 12.15.Lk, 13.85.Hd

I. INTRODUCTION

In 2007, the Large Hadron Collider (LHC) at CERN will begin operation. One of the main goals of the LHC experiments is to find the Higgs boson, or, more generally to unveil the mechanism of electroweak symmetry breaking. In order to discover the Higgs boson, or new physics, it is necessary to fully understand standard model (SM) processes. With the precision expected from LHC experiments, the theoretical uncertainties for many processes have to be reduced to the few percent level. In addition to the next-to-leading (NLO) and, in some cases, next-to-next-to-leading (NNLO) QCD corrections, this requires knowledge of the $\mathcal{O}(\alpha)$ electroweak (EW) radiative corrections.

The $\mathcal{O}(\alpha)$ virtual weak radiative corrections are known to become large and negative at high energies, due to the presence of Sudakov-like logarithms of the form $(\alpha/\pi)\log^2(\hat{s}/M_{W,Z}^2)$, where \hat{s} is the squared parton center of mass energy, and $M_{W,Z}$ is the mass of the W or Z boson. For $\sqrt{\hat{s}} \geq 1$ TeV, the $\mathcal{O}(\alpha)$ one-loop EW radiative corrections can easily become larger in magnitude than the $\mathcal{O}(\alpha_s)$ QCD corrections.

The source of the Sudakov-like logarithms is well understood [1–6]. They originate from collinear and infrared divergences which would be present in the limit of vanishing W and Z masses. In QED, these divergences are canceled by the corresponding divergences which originate from real photon radiation diagrams [7]. Because the underlying gauge symmetry is Abelian, observables which

include soft photons are infrared safe (Bloch-Nordsieck theorem) [8]. In non-Abelian gauge theories, the Bloch-Nordsieck theorem is violated. This was initially pointed out for QCD [9]. However, the infrared divergences present at the parton level in QCD have no practical consequences since one sums or averages over color charges when calculating physical observables. For electroweak interactions this is not automatically the case and large Sudakov-like logarithms may survive.

The appearance of large logarithms in one-loop weak corrections has been demonstrated in a number of explicit calculations. For hadron colliders, the $\mathcal{O}(\alpha)$ virtual weak corrections to inclusive jet [10], isolated photon [11,12], $Z + 1$ jet [12,13], Drell-Yan [14–19], di-boson [20–22], $\bar{t}t$ [23–26], and single top production [27–29] have been calculated. In almost all calculations, weak boson emission diagrams have not been taken into account, although they contribute at the same order in perturbation theory as the one-loop corrections. From the theoretical point of view this is justified. Since the W and Z masses act as infrared regulators, the weak boson emission diagrams are not necessary to obtain a finite answer (in contrast to QED or QCD corrections). Furthermore, since W and Z bosons decay, weak boson emission diagrams lead to a different final state.

Ignoring the contributions from weak boson emission thus is justified if a well-specified exclusive final state is considered. In experiment this is rarely the case. It is therefore necessary to carefully consider the role of weak boson emission when calculating the $\mathcal{O}(\alpha)$ EW radiative corrections to hadron collider processes. Qualitatively, one expects the cross section of weak boson emission processes

*Electronic address: baur@ubhex.physics.buffalo.edu

to grow asymptotically with $\log^2(\hat{s}/M_{W,Z}^2)$. In a hypothetical process where one sums/averages over all electroweak charges in the final/initial state, the $\log^2(\hat{s}/M_{W,Z}^2)$ terms arising from the $\mathcal{O}(\alpha)$ virtual weak corrections and from weak boson emission diagrams cancel at the parton level in the limit $\sqrt{\hat{s}} \gg M_{W,Z}$. In processes of practical interest, such as inclusive jet or isolated photon production, only a partial sum over the electroweak charges is performed, resulting in a partial cancellation of the $\mathcal{O}(\alpha)$ virtual weak corrections and the contributions from weak boson emission. Details depend on the process and the experimental requirements.

In this paper I examine in detail the role of weak boson emission in those hadron collider processes for which the $\mathcal{O}(\alpha)$ virtual weak corrections are known. In each case I determine how large the cross sections of the weak emission processes are compared with the Born cross section as a function of kinematic variables which are of experimental interest. Wherever possible, I compare these results with the effect of the $\mathcal{O}(\alpha)$ virtual weak corrections, the statistical and the (expected) systematic uncertainties.

In case of a charged final state with heavy quarks, weak boson emission can dramatically modify cross sections. This was pointed out in Ref. [29] for s -channel single top quark production at the LHC, $pp \rightarrow t\bar{b}, \bar{t}b$. While this process occurs to lowest order (LO) at $\mathcal{O}(\alpha^2)$, the corresponding W emission process, $pp \rightarrow t\bar{b}W^-, \bar{t}bW^+$ occurs at $\mathcal{O}(\alpha_s^2\alpha)$ and is completely dominated by $t\bar{t}$ production. I show that a similar phenomenon occurs in t -channel single top quark production. However, once realistic cuts are imposed, the effect of the gluon exchange diagrams is found to be small.

All tree-level (NLO QCD) cross sections in this paper are computed using CTEQ6L1 (CTEQ6M) [30] parton distribution functions (PDFs). For the CTEQ6L1 PDF's, the strong coupling constant is evaluated at leading order with $\alpha_s(M_Z^2) = 0.130$. The factorization and renormalization scales are set equal to M_Z . Since I mostly consider cross section ratios, results are quite insensitive to the choice of PDFs and the factorization and renormalization scales. The standard model (SM) parameters used in all tree-level calculations are [31]

$$G_\mu = 1.16639 \times 10^{-5} \text{ GeV}^{-2}, \quad (1)$$

$$M_Z = 91.188 \text{ GeV}, \quad M_W = 80.419 \text{ GeV}, \quad (2)$$

$$\sin^2\theta_W = 1 - \left(\frac{M_W^2}{M_Z^2}\right), \quad \alpha_{G_\mu} = \frac{\sqrt{2}}{\pi} G_F \sin^2\theta_W M_W^2, \quad (3)$$

where G_F is the Fermi constant, M_W and M_Z are the W and Z boson masses, θ_W is the weak mixing angle, and α_{G_μ} is the electromagnetic coupling constant in the G_μ scheme. I use the narrow width approximation for W, Z and top quark

decays, unless stated otherwise. Decay correlations are fully taken into account. Since I use the narrow width approximation, nonresonant diagrams which yield the same final state as W and Z boson emission with subsequent weak boson decay can be neglected. These diagrams formally contribute at one order higher in α than the weak boson emission diagrams.

In Sec. II I consider weak boson emission in QCD processes. Inclusive jet, isolated photon, and $Z + 1$ jet production are examined. Charged and neutral Drell-Yan production are studied in Sec. III. Weak boson emission in di-boson ($W\gamma, Z\gamma, WZ, ZZ$ and WW) production is calculated in Sec. IV, and in Sec. V this is done for $t\bar{t}$ and single top production. I summarize my findings in Sec. VI.

II. QCD PROCESSES

A. Inclusive jet production

The measurement of inclusive jet production in hadronic collisions constitutes a classic test of perturbative QCD. Recent experimental results from Run II of the Fermilab Tevatron are described in Refs. [32,33]. The lowest order process contributing to inclusive jet production is di-jet production at $\mathcal{O}(\alpha_s^2)$. The contributions from tree-level $\mathcal{O}(\alpha_s\alpha)$ and $\mathcal{O}(\alpha^2)$ diagrams [34] and the NLO QCD corrections to di-jet production [35] have been known for more than one decade. More recently, the $\mathcal{O}(\alpha)$ virtual weak corrections to di-jet production have been calculated and the tree-level $\mathcal{O}(\alpha_s\alpha)$ and $\mathcal{O}(\alpha^2)$ contributions were included in the calculation of the inclusive jet cross section [10]. Photonic corrections are not taken into account in this analysis.

For their analysis of inclusive jet production, the Tevatron experiments [32,33] select events which contain one or more isolated jets in a given transverse momentum (p_T) and pseudorapidity (η) range. There are no constraints on the number of electrons or muons in the event. However, in order to reduce the background from cosmic rays, events with large missing transverse momentum, \cancel{p}_T , are removed.

The experimental selection criteria imply that $\mathcal{O}(\alpha_s\alpha)$ $V + 1$ jet ($V = W^\pm, Z$) and $\mathcal{O}(\alpha_s^2\alpha)$ $V + 2$ jet production should be taken into account when calculating the cross section for inclusive jet production. Although events with $W \rightarrow \ell\nu$ ($\ell = e, \mu$) and $Z \rightarrow \bar{\nu}\nu$ are suppressed due to the \cancel{p}_T cut, those with $V \rightarrow jj$ fully contribute.

In order to properly take into account the associated production of weak bosons with jets up to $\mathcal{O}(\alpha_s^2\alpha)$, $V + 1$ jet production at NLO QCD has to be calculated. Utilizing the results of Ref. [36], I have evaluated the contribution of $V + 1$ jet production with $W \rightarrow \ell\nu, jj$ ($\ell = e, \mu, \tau$) and $Z \rightarrow \ell^+\ell^-, \bar{\nu}\nu, jj$ to the inclusive jet cross section at NLO in QCD. At least one jet with

$$p_T(j) > 25 \text{ GeV (Tevatron)}, \quad p_T(j) > 50 \text{ GeV (LHC)}, \quad (4)$$

and

$$|\eta(j)| < 2.5 \quad (5)$$

is required in the analysis. All jets satisfying Eqs. (4) and (5) have to be isolated from the other particles in the event, except neutrinos, by

$$\Delta R(j, X) > 0.4, \quad (6)$$

where $\Delta R = [(\Delta\phi)^2 + (\Delta\eta)^2]^{1/2}$ is the separation in pseudorapidity-azimuth space, and $X = j, \ell$. As cross checks, LO $V + 1$ jet and $V + 2$ jet production are calculated.

Here, and in all other calculations presented in this paper, τ -lepton decays are not taken into account. Since the branching ratios for $W \rightarrow \tau\nu$ and $Z \rightarrow \tau^+\tau^-$ are small, the approximation of treating τ -leptons on an equal footing with electrons and muons will change numerical results by at most a few percent. This is significantly less than the systematic uncertainties from the choice of PDFs, or the choice of the factorization or renormalization scale.

In Fig. 1, I show the ratio of the $Vj(j)$ and the $\mathcal{O}(\alpha_s^2)$ di-jet cross section for inclusive jet production as a function of the jet transverse momentum at the Tevatron and the LHC. In events with more than one jet satisfying Eqs. (4) and (5), each jet contributes, i.e. such events produce multiple entries in the distribution. Since the \cancel{p}_T veto imposed depends on experimental details, I show results for two extreme cases: no \cancel{p}_T veto (solid line) and removing all events with nonzero \cancel{p}_T (dashed line). For a realistic \cancel{p}_T veto, the result will fall somewhere in between the two lines.

At the Tevatron (LHC), the $Vj(j)$ to LO di-jet cross section ratio asymptotically approaches 0.6%–1.0% (4.5%–6.5%) at large values of $p_T(j)$. $V + 1$ jet production contributes significantly only for $p_T(j) < 200$ –300 GeV; for large jet transverse momenta Vjj production dominates. This is to be expected: at large values of $p_T(j)$, soft and collinear logarithms appear in Vjj production.

This is not the case in $p\bar{p} \rightarrow Vj$, where the W or Z boson balances the jet in transverse momentum. At very large jet transverse momentum, the separation cut of Eq. (6) limits the relative growth of the $Vj(j)$ cross section.

The calculation performed here approximates the QCD corrections associated with the hadronic decays of the W or Z boson by using a branching fraction for $V \rightarrow jj$ which takes into account NLO QCD corrections. This approximation does not correctly treat contributions from Vj production with $V \rightarrow jjj$. A correct treatment of the final state QCD corrections is expected to modify the result presented here at the 10%–30% level for $p_T(j) < 200$ GeV, but will have a negligible effect at higher jet transverse momenta. Note that, except for $p_T(j) < M_V/2$, contributions from $p\bar{p} \rightarrow V \rightarrow 4j$ are also negligible

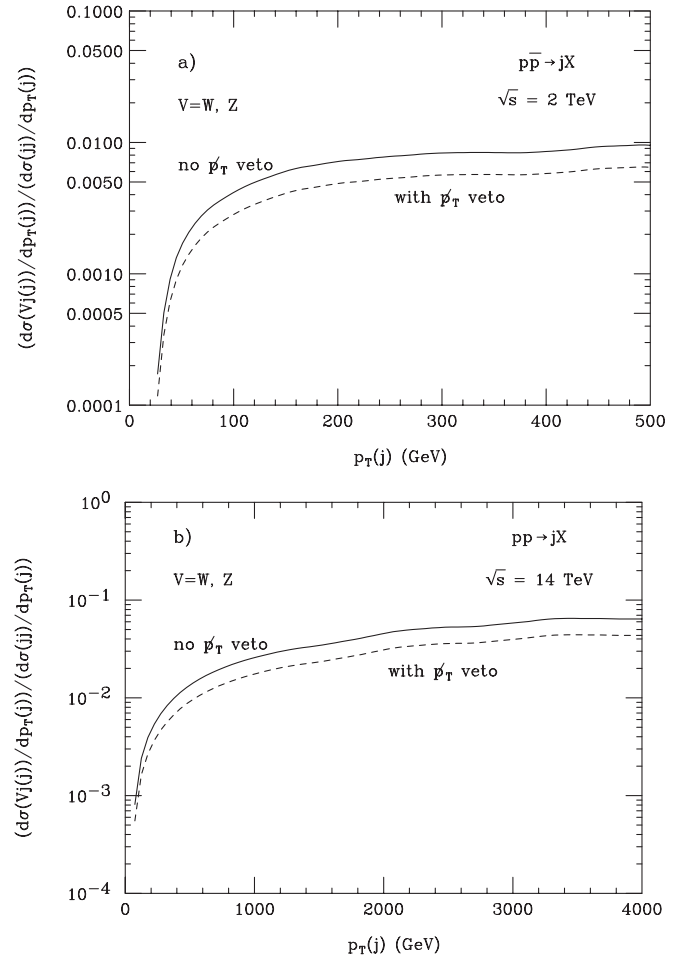


FIG. 1. Ratio of the NLO QCD Vj ($V = W^\pm, Z; W \rightarrow \ell\nu, jj, Z \rightarrow \ell^+\ell^-, \bar{\nu}\nu, jj$) and the $\mathcal{O}(\alpha_s^2)$ di-jet cross section for inclusive jet production as a function of the jet transverse momentum (a) at the Tevatron, and (b) at the LHC. Results are shown for two extreme cases: with no \cancel{p}_T veto imposed (solid line), and removing all events with nonzero \cancel{p}_T (dashed line). The cuts imposed are described in the text.

[they are of $\mathcal{O}(\alpha_s^2\alpha^2)$]. They are not included in the calculation presented here.

The contributions of the weak boson emission processes $p\bar{p} \rightarrow Vj(j)$ to the inclusive jet cross section should be compared with those of the tree-level $\mathcal{O}(\alpha_s\alpha + \alpha^2)$ diagrams and the $\mathcal{O}(\alpha)$ virtual weak corrections calculated in Ref. [10]. Since I am using somewhat different input parameters, an exact comparison is not possible. Nevertheless, it is instructive to list the relative size of the $Vj(j)$ contributions, $\delta(Vj(j))$, and the combined tree level $\mathcal{O}(\alpha_s\alpha + \alpha^2)$ and the $\mathcal{O}(\alpha_s^2\alpha)$ virtual one-loop weak corrections, δ (1-loop), side-by-side. The results are shown in Table I.

As expected, the contributions from weak boson emission partially cancel the effects of the one-loop virtual weak corrections. At the Tevatron, at small jet transverse momenta, $\delta(Vj(j))$ and δ (1-loop) approximately cancel.

TABLE I. Relative size of the $Vj(j)$ contributions, $\delta(Vj(j))$, and the combined tree-level $\mathcal{O}(\alpha_s\alpha + \alpha^2)$ and the $\mathcal{O}(\alpha_s^2\alpha)$ virtual one-loop weak corrections, δ (1-loop), to inclusive jet production at the Tevatron and LHC as a function of the jet transverse momentum. Cross sections are normalized to the $\mathcal{O}(\alpha_s^2)$ cross section. The results for the tree-level $\mathcal{O}(\alpha_s\alpha + \alpha^2)$ and $\mathcal{O}(\alpha_s^2\alpha)$ one-loop virtual weak corrections are taken from Ref. [10]. Results for $\delta(Vj(j))$ with a \not{p}_T veto are given in parenthesis.

Tevatron			LHC		
$p_T(j)$ (GeV)	δ (1-loop) (%)	$\delta(Vj(j))$ (%)	$p_T(j)$ (GeV)	δ (1-loop) (%)	$\delta(Vj(j))$ (%)
100	-0.36	0.41 (0.28)	1000	-9	2.5 (1.7)
550	-6.9	1.1 (0.73)	4000	-24	6.5 (4.4)

At large values of $p_T(j)$, weak boson emission reduces the effect of the $\mathcal{O}(\alpha)$ virtual weak corrections and the tree-level $\mathcal{O}(\alpha_s\alpha + \alpha^2)$ diagrams by 10%–13%. At the LHC, weak boson emission diagrams play a larger role; here $\delta(Vj(j))/\delta$ (1-loop) is in the range 0.2–0.3.

In order to determine whether the combined effect of the $\mathcal{O}(\alpha)$ virtual weak corrections and the contributions from tree level $\mathcal{O}(\alpha_s\alpha + \alpha^2)$ and weak boson emission diagrams need to be taken into account for the analysis of Tevatron and LHC inclusive jet data, the results shown in Table I have to be compared with the statistical, systematic and other theoretical uncertainties. At the Tevatron, the systematic and PDF uncertainties increase from about 10% at low $p_T(j)$ to $\sim 40\%$ at $p_T(j) = 500$ GeV [32,33]. Uncertainties from higher order QCD corrections are $\leq 10\%$ for the $p_T(j)$ range considered [33]. Except for the highest jet transverse momenta, electroweak corrections thus should be negligible at the Tevatron. At the LHC one expects systematic and PDF uncertainties of 10%–20% each for $p_T(j) \leq 1$ TeV, and $\sim 50\%$ at $p_T(j) = 4$ TeV [37], the highest jet p_T which can be reached with an integrated luminosity of 100 fb^{-1} . Electroweak radiative corrections to inclusive jet production thus will be relevant for data analysis at the LHC.

B. Isolated photon production

Isolated photon production in hadronic collisions has been another important tool for probing QCD in the past. It has also presented theoretical challenges, in particular, at fixed target energies (see Ref. [38] for a recent theoretical review). The most recent measurements of the Tevatron experiments are described in Refs. [39,40]. The lowest order process contributing to isolated photon production is $p\bar{p} \rightarrow \gamma j$ at $\mathcal{O}(\alpha_s\alpha)$.

For their isolated photon analysis, the Tevatron experiments select events with a high p_T , isolated photon. Backgrounds from cosmic rays and W decays are reduced by rejecting events with large \not{p}_T . There are no requirements on the number of charged leptons or jets in the event. In the following, I assume that similar selection criteria will be used at the LHC.

The $\mathcal{O}(\alpha)$ virtual weak corrections to $p\bar{p} \rightarrow \gamma j$ were calculated in Refs. [11,12]. Since there are no restrictions on the number of jets or charged leptons in isolated photon

events, tree-level $\mathcal{O}(\alpha_s\alpha^2)$ $V\gamma j$ ($V = W^\pm, Z$) production should be included in the calculation. Likewise, $\mathcal{O}(\alpha^2)$ $V\gamma$ production should also be taken into account. $V\gamma j$ production is known to exhibit a logarithmic enhancement factor which is similar to that found in the $\mathcal{O}(\alpha)$ virtual weak corrections. In the limit of large photon transverse momenta, $p_T(\gamma) \gg M_V$, the $q_1 g \rightarrow V\gamma q_{1,2}$ differential cross section can be written in the form [41,42]

$$d\hat{\sigma}(q_1 g \rightarrow V\gamma q_{1,2}) = d\hat{\sigma}(q_1 g \rightarrow \gamma q_1) \frac{\alpha}{4\pi \sin^2\theta_W} \times \log^2\left(\frac{p_T^2(\gamma)}{M_V^2}\right). \quad (7)$$

The $V\gamma j$ and $V\gamma$ contributions can be taken into account simultaneously by computing the $p\bar{p} \rightarrow \gamma j$ cross section including NLO QCD corrections. Using the results of [42–44] I have calculated how NLO QCD $V\gamma$ production modifies the isolated photon cross section at the Tevatron and LHC. Figure 2 shows the relative correction $\mathcal{R}_{\gamma j}(p_T(\gamma))$ with respect to the LO γj cross section as a function of the photon transverse momentum. Here, the relative correction is defined as

$$\mathcal{R}_Y(X) = \frac{d\sigma/dX}{d\sigma^{\text{LO}}(Y)/dX} - 1 \quad (8)$$

with X being the kinematic variable considered, and Y the final state of the LO process.

In Fig. 2, photons are required to have

$$|\eta(\gamma)| < 2.5 \quad (9)$$

and be isolated from jets and charged leptons by a distance

$$\Delta R(\gamma, j) > 0.4, \quad \Delta R(\gamma, \ell) > 0.4. \quad (10)$$

The blue curve shows $\mathcal{R}_{\gamma j}(p_T(\gamma))$ if only the $\mathcal{O}(\alpha)$ virtual weak corrections [11,12] are taken into account. It has been obtained by incorporating the leading $\mathcal{O}(\alpha)$ virtual weak corrections of Ref. [11] into a parton level $p\bar{p} \rightarrow \gamma j$ Monte Carlo program, and by parametrizing the remaining corrections.

The solid black curve in Fig. 2 displays the result if NLO QCD $V\gamma$ production with $V \rightarrow jj$, $W \rightarrow \ell\nu$, $Z \rightarrow \ell^+\ell^-$ and $Z \rightarrow \bar{\nu}\nu$ is also included and no \not{p}_T veto is imposed. The dashed curve finally shows the relative correction if

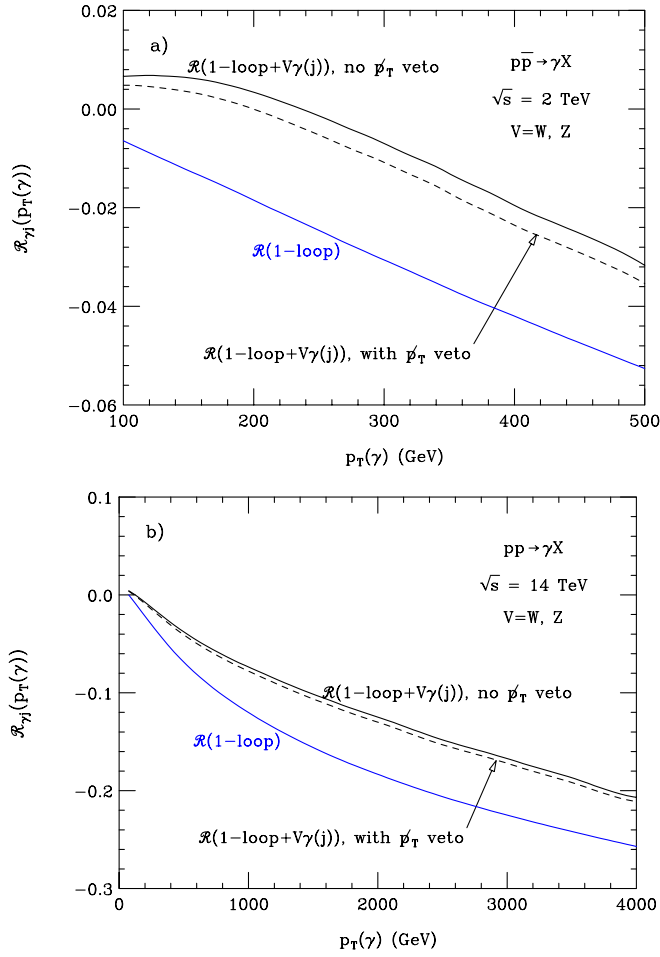


FIG. 2 (color online). Relative correction with respect to the LO γj cross section, $\mathcal{R}_{\gamma j}$, as a function of the photon transverse momentum, $p_T(\gamma)$, for a) the Tevatron and b) the LHC. The blue curve shows the result if only the $\mathcal{O}(\alpha)$ virtual weak corrections of Ref. [11] are taken into account. The black dashed (solid) curve shows \mathcal{R} if in addition $V\gamma(j)$ production is included and a (no) \cancel{p}_T veto is imposed. The definition of \mathcal{R} and the cuts imposed are described in the text.

both $\mathcal{O}(\alpha)$ virtual weak corrections and NLO QCD $V\gamma$ production are included, however, events are required to have

$$\cancel{p}_T \leq 5 \text{ GeV}^{1/2} \sqrt{\sum p_T}. \quad (11)$$

Here the sum extends over all particles except neutrinos. The \cancel{p}_T veto is seen to have only a relatively small effect.

Since the $V\gamma$ two body final state does not have any soft or collinear enhancement factors, it contributes significantly only for $p_T(\gamma) \leq 200\text{--}300$ GeV. This is also the case for $V\gamma$ production with $V \rightarrow jjj$, which is not included in the calculation presented here.

Figure 2(a) shows that, at the Tevatron, weak boson emission effects in isolated photon production essentially cancel the corrections from the $\mathcal{O}(\alpha)$ virtual weak dia-

grams for photon transverse momenta up to about 200 GeV. At $p_T(\gamma) = 500$ GeV, they reduce $\mathcal{R}_{\gamma j}(p_T(\gamma))$ from -5.2% to $-(3.2\text{--}3.5)\%$, i.e. by 30%–40%.

At the LHC, with an integrated luminosity of 10 fb^{-1} (100 fb^{-1}), it should be possible to measure the photon transverse momentum distribution for values up to 1.5 TeV (2.0 TeV). For $p_T(\gamma) = 2.0$ TeV, the combined $\mathcal{O}(\alpha)$ virtual weak corrections and weak boson emission effects reduce the LO γj cross section by about 13%, compared with 19% if the $V\gamma j$ diagrams are ignored [see Fig. 2(b)]. The leading $\mathcal{O}(\alpha_s \alpha^3)$ two-loop weak corrections [11] and $\mathcal{O}(\alpha_s \alpha^2)$ weak boson emission have a very similar numerical effect on the isolated photon cross section. Thus, when the leading $\mathcal{O}(\alpha_s \alpha^3)$ two-loop weak corrections are also taken into account, weak radiative corrections reduce the LO γj cross section only by about 7% at $p_T(\gamma) = 2.0$ TeV.

At the Tevatron, the combined $\mathcal{O}(\alpha)$ virtual weak corrections and contributions from weak boson emission do not exceed 3.5% for photon transverse momenta $p_T(\gamma) \leq 500$ GeV. The current D0 Run II analysis [40] covers the region $p_T(\gamma) \leq 300$ GeV. In this region the systematic error varies between 10% and 20%, and is always larger than the statistical uncertainty. The systematic uncertainty decreases with increasing photon transverse momentum. Weak radiative corrections thus will not be important in isolated photon production at the Tevatron. So far, there are no estimates of the systematic uncertainties in $pp \rightarrow \gamma X$ at the LHC. However, the results shown in Fig. 2(b) show that, unless the systematic uncertainties are much larger than at the Tevatron, weak radiative corrections should be taken into account when analyzing isolated photon production at the LHC.

Weak boson emission effects would be very much reduced if one were to measure the cross section for exclusive $\gamma + 1$ jet production instead of the inclusive isolated photon cross section. $\gamma + 1$ jet production may be useful for calibrating jet energies at the LHC [45].

C. $Z + 1$ jet production

$Z + 1$ jet production is the dominant contribution to Z boson production at large transverse momentum. The Tevatron experiments have not yet reported results on the $p_T(Z)$ distribution for $p_T(Z) > 50$ GeV from Run II. Run I measurements are described in Refs. [46,47]. Z boson events are selected by requiring an e^+e^- pair which is consistent in invariant mass with a Z boson. In a measurement of the transverse momentum distribution of the Z boson no requirements on the number of jets in the event are made. However, events with more than two charged leptons are rejected as di-boson candidates.

The $\mathcal{O}(\alpha)$ virtual weak corrections to $Z + 1$ jet production were calculated in Refs. [12,13]. Z boson decays were not taken into account in this calculation. Since the number of jets is not fixed in a measurement of the Z boson

transverse momentum, $\mathcal{O}(\alpha_s\alpha^2)$ ZVj production with $V \rightarrow jj$ has to be included when calculating weak radiative corrections to the Z boson transverse momentum distribution. ZZj events with one Z boson decaying into neutrinos may also contribute, depending on whether events with a substantial amount of \cancel{p}_T are allowed by the experimental selection criteria or not. Similar to the situation encountered in inclusive jet and isolated photon production, a more complete treatment includes the contributions from ZV , $V \rightarrow jj$ production, and utilizes a calculation which includes the NLO QCD corrections to these processes. To

compute the contributions of $p\bar{p} \rightarrow ZV$ at NLO QCD, I have used the results of Refs. [48] in the WZ case, and those of Ref. [49], as implemented in MCFM-5.1 [50], for ZZ production. These calculations assume that both weak bosons decay leptonically. To estimate NLO QCD ZV , $V \rightarrow jj$, production, I rescale the cross section obtained for leptonic V decays to correct for the higher $V \rightarrow jj$ branching ratio. This approximation does not correctly treat final state NLO QCD corrections, in particular ZV production with $V \rightarrow jjj$. However, similar to the situation encountered in inclusive jet and isolated photon production, final state QCD corrections to ZV production are expected to have a non-negligible effect only at small values of $p_T(Z)$.

The relative correction, $\mathcal{R}_{Zj}(p_T(Z))$ [see Eq. (8)], to the lowest order $Z + 1$ jet cross section is shown in Fig. 3. Here I require that events contain at least one jet with

$$p_T(j) > 25 \text{ GeV (Tevatron)}, \quad p_T(j) > 50 \text{ GeV (LHC)}, \quad (12)$$

and

$$|\eta(j)| < 2.5. \quad (13)$$

In addition I impose the \cancel{p}_T veto of Eq. (11). Since Z boson decays were not taken into account in Refs. [12,13], I treat the Z boson as a stable particle in this calculation.

The solid curve shows the result taking only the $\mathcal{O}(\alpha)$ virtual weak corrections [12,13] into account. It has been obtained by incorporating the leading $\mathcal{O}(\alpha)$ virtual weak corrections of Ref. [13] into a parton level $p\bar{p} \rightarrow Zj$ Monte Carlo program, and by parameterizing the remaining corrections. The dashed line displays $\mathcal{R}_{Zj}(p_T(Z))$ if $ZV(j)$ production with $V \rightarrow jj$ is also included in the calculation. The two-body process $p\bar{p} \rightarrow ZV$ contributes significantly only for small Z boson transverse momenta.

The $\mathcal{O}(\alpha)$ virtual weak corrections to $Z + 1$ jet production are considerably larger than those found for isolated photon production. At the Tevatron, weak boson emission increases $\mathcal{R}_{Zj}(p_T(Z))$ by about 2% over the p_T range studied here. In Run II, CDF and D0 should be able to map out the $p_T(Z)$ distribution up to transverse momenta of 350–400 GeV. In this range, the full $\mathcal{O}(\alpha)$ weak correc-

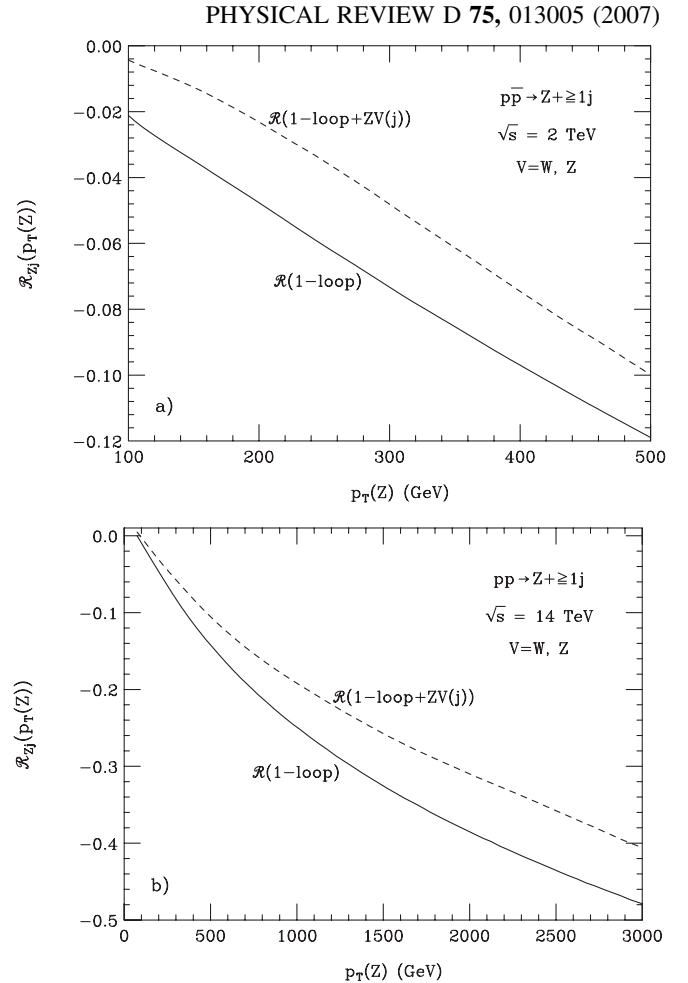


FIG. 3. Relative correction with respect to the LO $Z + 1$ jet cross section, \mathcal{R}_{Zj} , as a function of the Z boson transverse momentum, $p_T(Z)$, for (a) the Tevatron and (b) the LHC. The solid curve shows the result if only the $\mathcal{O}(\alpha)$ virtual weak corrections of Ref. [13] are taken into account. The dashed curve shows $\mathcal{R}_{Zj}(p_T(Z))$ if $ZV(j)$ production with $V \rightarrow jj$ is included as well. The definition of $\mathcal{R}_{Zj}(p_T(Z))$ and the cuts imposed are described in the text.

tions reduce the LO $Z + 1$ jet cross section by 6%–8%. The weak radiative corrections are thus of the same size as the expected systematic uncertainties [46,47] which should dominate over the statistical errors except for the very highest $p_T(Z)$ bin.

At the LHC, with $Z \rightarrow e^+e^-$, transverse momenta up to 1.0 TeV (1.5 TeV) can be reached with an integrated luminosity of 10 fb^{-1} (100 fb^{-1}). For $p_T(Z) = 1.5$ TeV, the $\mathcal{O}(\alpha)$ virtual weak corrections reduce the LO $Z + 1$ jet cross section by about 33%. Including weak boson emission decreases the magnitude of \mathcal{R}_{Zj} to 27%. W and Z boson radiation and the leading two-loop weak corrections [13] have a very similar effect on the $Z + 1$ jet cross section at LHC energies. The systematic uncertainties at the LHC and the Tevatron are expected to be similar [37]. It will thus be important to take into account the full $\mathcal{O}(\alpha)$

weak corrections, including weak boson emission diagrams, at both the Tevatron and the LHC.

III. DRELL-YAN PRODUCTION

Charged and neutral Drell-Yan production, $p p^{(-)} \rightarrow \ell \nu$ and $p p^{(-)} \rightarrow \ell^+ \ell^-$, at masses and transverse momenta larger than the W or Z mass, are tools to search for new heavy gauge bosons [51], W' and Z' , and other resonances, such as gravitons in Randall-Sundrum models [52]. The most recent Tevatron Run II results for W' , Z' , and graviton searches are described in Refs. [53–55]. In the charged channel, events are selected by requiring one charged lepton and large missing transverse momentum. In the neutral channel, two oppositely charged leptons are required, and no significant amount of \cancel{p}_T is allowed. The number of jets in the event is not restricted in both the charged and the neutral channel. Weak boson emission, i.e. $\ell \nu V$ and $\ell^+ \ell^- V$ production with $V \rightarrow jj$, may thus contribute to Drell-Yan production at $\mathcal{O}(\alpha^3)$. In the charged channel, $p p^{(-)} \rightarrow \ell \nu Z$ with $Z \rightarrow \bar{\nu} \nu$ may also play a role.

The $\mathcal{O}(\alpha)$ EW radiative corrections to $p p^{(-)} \rightarrow \ell \nu$ and $p p^{(-)} \rightarrow \ell^+ \ell^-$ were calculated in [14–19]. In the following, I shall use the calculations of Refs. [14,16]. In addition to the weak one-loop corrections, these calculations also take into account photonic corrections.

The granularity of detectors and the size of electromagnetic showers in the calorimeter make it difficult to discriminate between electrons and photons with a small opening angle. In such cases, the four-momentum vectors of the electron and photon are recombined to an effective electron four-momentum vector. The exact recombination procedure is detector dependent. Recombining the electron and photon four-momentum vectors eliminates the mass singular logarithmic terms originating from final state photon radiation and strongly reduces the size of the photonic final state corrections [56].

Muons are identified by hits in the muon chambers and the requirement that the associated track is consistent with a minimum ionizing particle. This limits the photon energy for small muon-photon opening angles. The cut on the photon energy increases the size of the photonic corrections. The photonic corrections are not of interest for the following discussion. I therefore focus on final states containing electrons and impose realistic electron identification requirements. This minimizes the effect of the photonic corrections. For $M_T > 150$ GeV and $p_T(e) > 80$ GeV, the one-loop weak correction dominates over the photonic corrections.

In the calculations presented in this Section, electrons are required to have

$$p_T(e) > 25 \text{ GeV} \quad \text{and} \quad |\eta(e)| < 2.5. \quad (14)$$

The electron identification requirements are taken from

Ref. [16]. Electrons also have to be isolated from the hadronic decay products in $e \nu V$ and $e^+ e^- V$ events with $V \rightarrow jj$:

$$\Delta R(e, j) > 0.4. \quad (15)$$

In the charged channel, events also must have

$$\cancel{p}_T > 25 \text{ GeV}, \quad (16)$$

whereas the \cancel{p}_T veto of Eq. (11) is imposed in the neutral channel. The cross sections for $p p^{(-)} \rightarrow e \nu V$, $e^+ e^- V$ with $V \rightarrow jj$ are calculated using MADEVENT [57]. For $e \nu Z$ and $e^+ e^- Z$ production with $Z \rightarrow \bar{\nu} \nu$, the calculation is based on the complete set of tree-level Feynman diagrams contributing to the $e \nu_e \bar{\nu}_\ell \nu_\ell$ final state ($\ell = e, \mu, \tau$).

The relative correction to the cross section in the charged channel as a function of the $e \nu$ transverse mass,

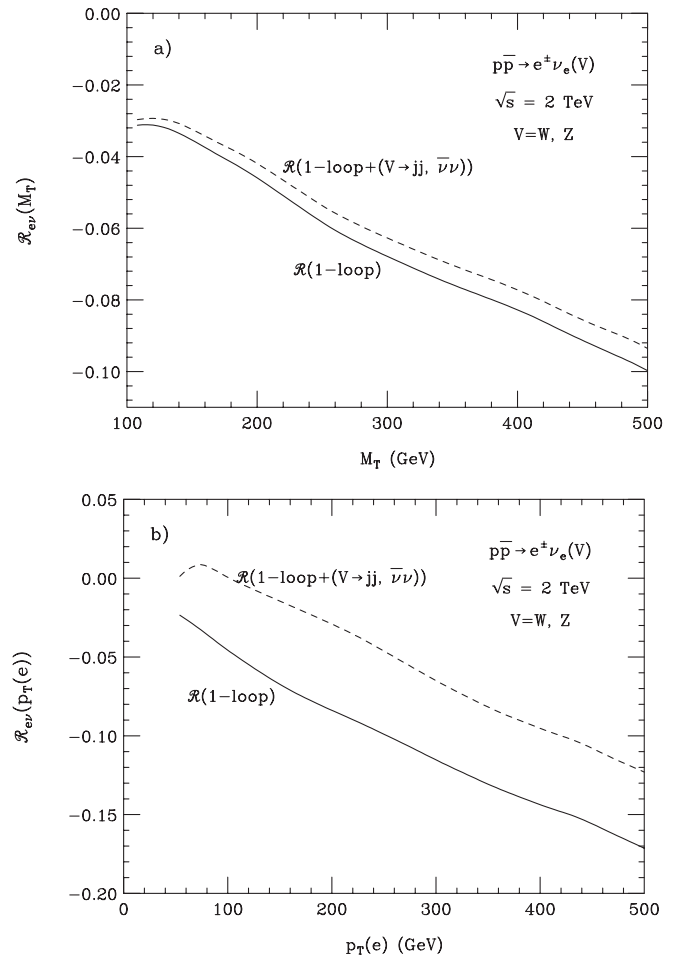


FIG. 4. The relative correction with respect to the LO $e \nu$ cross section at the Tevatron as a function (a) of the $e \nu$ transverse mass and (b) the electron p_T . The solid curve shows the result if only the $\mathcal{O}(\alpha)$ corrections of Ref. [16] are taken into account. The dashed curve shows \mathcal{R}_{ev} if $\mathcal{O}(\alpha^3)$ $e \nu V$ production with $V \rightarrow jj$ and $Z \rightarrow \bar{\nu} \nu$ is included as well. The definition of \mathcal{R}_{ev} and the cuts imposed are described in the text.

M_T , and the electron transverse momentum, $p_T(e)$, is shown in Fig. 4. The transverse mass is defined by

$$M_T = \sqrt{2p_T(e)\cancel{p}_T(1 - \cos\phi^{e\cancel{p}_T})}, \quad (17)$$

where $\phi^{e\cancel{p}_T}$ is the angle between the electron and the missing transverse momentum vector in the transverse plane. The solid line in Fig. 4 shows the result for $\mathcal{R}_{e\nu}$ for the one-loop weak and photonic $\mathcal{O}(\alpha)$ corrections of Ref. [16]. In the dashed line, the $e\nu V$ contributions with $V \rightarrow jj$ and $Z \rightarrow \bar{\nu}\nu$ are also included.

Figure 4(a) shows that weak boson emission effects in the M_T distribution are quite small at the Tevatron. They increase $\mathcal{R}_{e\nu}$ by less than 0.01 for the M_T range considered here. The effect of the weak boson emission diagrams is much more pronounced in the electron transverse momen-

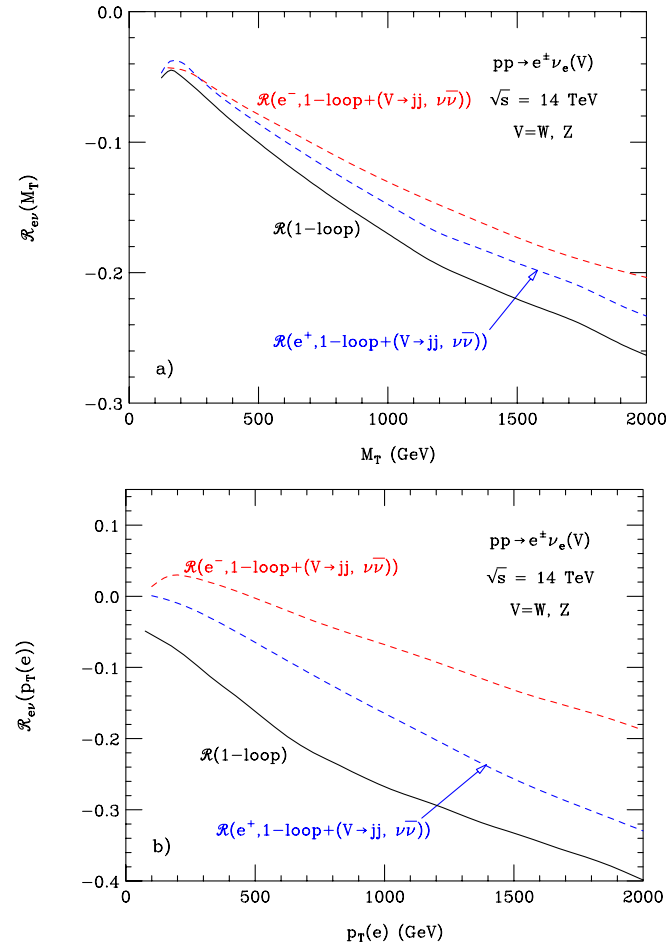


FIG. 5 (color online). The relative correction with respect to the LO $e\nu$ cross section at the LHC as a function (a) of the $e\nu$ transverse mass and (b) the electron p_T . The solid line shows the result if only the $\mathcal{O}(\alpha)$ corrections of Ref. [16] are taken into account. The dashed blue (red) curve shows $\mathcal{R}_{e\nu}$ in the $e^+ \nu$ ($e^- \bar{\nu}$) channel if $\mathcal{O}(\alpha^3)$ $e\nu V$ production with $V \rightarrow jj$ and $Z \rightarrow \bar{\nu}\nu$ is included in addition. The definition of $\mathcal{R}_{e\nu}$ and the cuts imposed are described in the text.

tum distribution. For $p_T(e) > 100$ GeV, W and Z radiation increases $\mathcal{R}_{e\nu}$ uniformly by about 0.05. The $\mathcal{O}(\alpha)$ weak one-loop corrections and the contribution from weak boson emission thus cancel to a significant degree in the $p_T(e)$ distribution. It is easy to understand why W and Z radiation has a larger effect in the electron transverse momentum distribution. Since $M_T \leq m(e\nu)$, where $m(e\nu)$ is the $e\nu$ invariant mass, $m(e\nu)$ is always well above the W resonance region for the M_T range studied here. On the other hand, for large $p_T(e)$, the transverse momenta of the electron and the W or Z boson radiated in the event can balance, and the neutrino can be relatively soft. In this kinematic configuration, the $e\nu$ system can form an on-shell W . In a nutshell, in the $p_T(e)$ distribution, on-shell WV production contributes, while it does not in the transverse mass distribution (for $M_T > 100$ GeV).

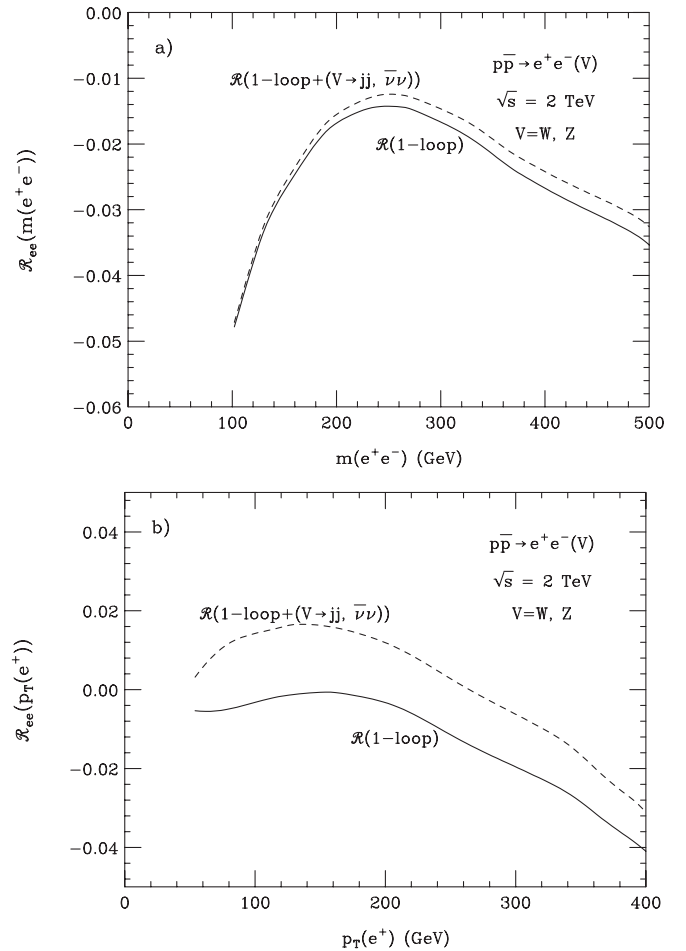


FIG. 6. The relative correction with respect to the LO e^+e^- cross section at the Tevatron as a function (a) of the e^+e^- invariant mass and (b) the positron p_T . The solid curve shows the result if only the $\mathcal{O}(\alpha)$ corrections of Ref. [14] are taken into account. The dashed curve shows \mathcal{R}_{ee} if $\mathcal{O}(\alpha^3)$ $e^+e^- V$ production with $V \rightarrow jj$ and $Z \rightarrow \bar{\nu}\nu$ is included as well. The definition of \mathcal{R}_{ee} and the cuts imposed are described in the text.

$\mathcal{R}_{e\nu}$ as a function of M_T and $p_T(e)$ at the LHC is shown in Fig. 5. As at the Tevatron, weak boson emission effects are more pronounced in the electron transverse momentum distribution. At the LHC, the cross sections for $e^+\nu$ and $e^-\bar{\nu}$ production are different. At large values of M_T and $p_T(e)$, the $e^+\nu$ cross section is almost one order magnitude larger. Since the weak one-loop corrections are proportional to the LO $e^\pm\nu$ cross section and the photonic corrections are dominated by final state radiation effects, the relative corrections to the $e^+\nu$ and $e^-\bar{\nu}$ cross sections due to these effects are almost equal. They are represented by the black solid lines in Fig. 5. Weak boson emission effects are dominated by $e^\pm\nu W^\pm$ production which yield equal cross sections in the two cases. Since the LO $e^-\bar{\nu}$ cross section is much smaller than the LO $e^+\nu$ rate, W radiation affects $\mathcal{R}_{e\nu}$ much more strongly in the $e^-\bar{\nu}$ channel.

At $p_T(e) = 1.0$ TeV, weak boson emission reduces $\mathcal{R}_{e\nu}$ from 28% to 7% (17%) in magnitude for $e^-\bar{\nu}$ ($e^+\nu$)

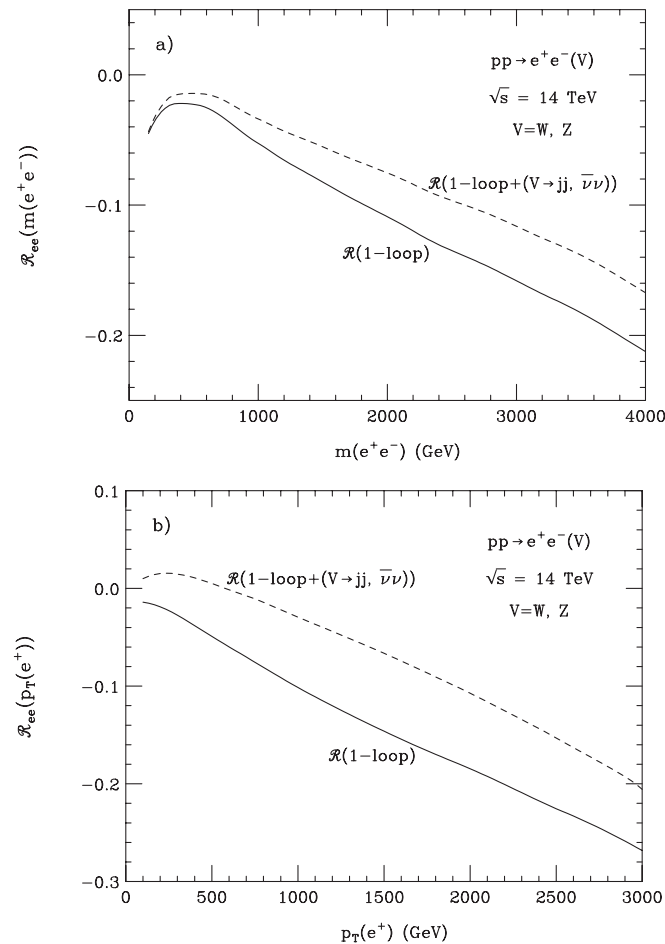


FIG. 7. The relative correction with respect to the LO e^+e^- cross section at the LHC as a function of (a) of the e^+e^- invariant mass and (b) the positron p_T . The solid curve shows the result if only the $\mathcal{O}(\alpha)$ corrections of Ref. [14] are taken into account. The dashed curve shows \mathcal{R}_{ee} if $\mathcal{O}(\alpha^3)$ e^+e^-V production with $V \rightarrow jj$ and $Z \rightarrow \bar{\nu}\nu$ is included as well. The definition of \mathcal{R}_{ee} and the cuts imposed are described in the text.

production. For an integrated luminosity of 100 fb^{-1} , one expects to measure the $p_T(e)$ (M_T) distribution for values up to 1 TeV (2 TeV).

Results for the neutral channel are shown in Fig. 6 for the Tevatron, and in Fig. 7 for the LHC. To calculate the relative correction to the LO e^+e^- cross section which originate from the $\mathcal{O}(\alpha)$ weak one-loop and photonic corrections, I have used the results of Ref. [14]. The one-loop weak corrections in neutral Drell-Yan production are seen to have a smaller effect on the differential cross section than in the charged channel. As in $e\nu$ production, weak boson emission effects in the neutral channel are quite small at the Tevatron. They increase \mathcal{R}_{ee} by less than 0.01 over most of the invariant mass and p_T ranges considered. At the LHC, W and Z radiation increase \mathcal{R}_{ee} by up to 0.06. For example, at $m(e^+e^-) = 2.0$ TeV, the relative correction to the differential cross section without (with) weak boson emission is $\mathcal{R}_{ee}(m(e^+e^-)) = -0.108$ [$\mathcal{R}_{ee}(m(e^+e^-)) = -0.073$]. For comparison, the statistical uncertainty of the Drell-Yan cross section at $m(e^+e^-) = 2.0$ TeV is about 18% for 100 fb^{-1} . W and Z radiation thus moderately reduce the size of the $\mathcal{O}(\alpha)$ electroweak radiative corrections to the neutral Drell-Yan cross section at the LHC in the experimentally accessible invariant mass range.

The experimental and theoretical systematic uncertainties in charged and neutral Drell-Yan production at the Tevatron are of $\mathcal{O}(10\%)$ [53–55]. A similar result is expected at the LHC [37,58]. Therefore, with the possible exception of neutral Drell-Yan production at the Tevatron, electroweak radiative corrections and weak boson emission will have a non-negligible effect.

IV. DI-BOSON PRODUCTION

Di-boson production, $p\bar{p} \rightarrow W^\pm\gamma, Z\gamma, W^\pm Z, ZZ, W^+W^-$, offers an opportunity to probe the gauge boson self-couplings [59]. At the LHC, W^+W^- and ZZ production are also of interest as background processes to Higgs boson production [60]. In order to precisely measure the gauge boson self-couplings, accurate theoretical predictions are needed. The NLO QCD corrections to di-boson production have been calculated several years ago [41–44,48,61]. More recently, the combined one-loop weak and photonic corrections to these processes have been computed [20–22]. Contributions from weak boson emission are not included in these calculations. Furthermore, numerical results are presented only for the LHC. In the following, I therefore consider di-boson production only at the LHC.

The experimental systematic and the PDF uncertainties at the LHC for all di-boson production processes are in the 5%–15% range [37,62]. The uncertainty from higher order QCD corrections for the individual processes is discussed in more detail below.

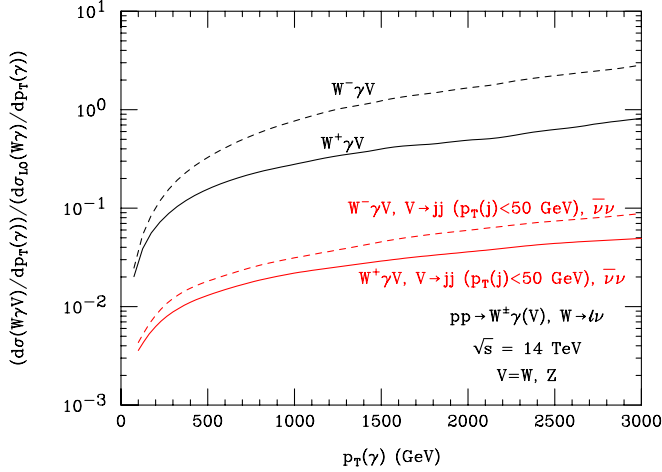


FIG. 8 (color online). Ratio of the $W\gamma V$ ($V = W^\pm, Z$) and the LO $W\gamma$ cross section as a function of the photon transverse momentum at the LHC. The W boson is required to decay leptonically. Results are shown for the inclusive case (black solid and dashed lines), and for the case where jets with $p_T(j) > 50$ GeV and $|\eta(j)| < 4.5$, and events with more than one charged lepton, are vetoed (red solid and dashed lines). The cuts imposed are listed in Eqs. (18)–(20).

A. $W\gamma$ and $Z\gamma$ production

$W\gamma$ events are usually selected by requiring the W boson to decay leptonically. For hadronic W decays, QCD γjj production constitutes a very large background. To identify $W\gamma$ events, experiments therefore search for events with one isolated high p_T charged lepton, large missing transverse momentum, and an isolated hard photon. To be specific, I impose the following cuts in the calculation of the $W\gamma$ cross section at the LHC:

$$p_T(\ell) > 25 \text{ GeV}, \quad |\eta(\ell)| < 2.5, \quad (18)$$

$$p_T(\gamma) > 50 \text{ GeV}, \quad |\eta(\gamma)| < 2.5, \quad (19)$$

$$\cancel{p}_T > 25 \text{ GeV} \quad \text{and} \quad \Delta R(\ell\gamma) > 0.4. \quad (20)$$

Because of the relatively large photon p_T cut, radiative W decay, $pp \rightarrow W \rightarrow \ell\nu\gamma$ is strongly suppressed and henceforth will be ignored. To compute weak boson emission

effects in $W\gamma$ production, the cross sections for $pp \rightarrow W\gamma V$ ($V = W^\pm, Z$) have to be calculated.

Before discussing which V decays should be considered, it is instructive to consider the ratio of the $W\gamma V$ and the LO $\mathcal{O}(\alpha^2)$ $W\gamma$ cross section in the inclusive $V \rightarrow$ all case with no cuts imposed on the V decay products. This ratio is shown as a function of the photon transverse momentum in Fig. 8 (black solid and dashed lines). Since anomalous $WW\gamma$ couplings lead to large deviations at high values of photon p_T , the transverse momentum distribution of the photon is of particular interest in $W\gamma$ production. With 100 fb^{-1} , $W\gamma$ events with a photon p_T up to about 1 TeV will be produced. For inclusive V decays, the $W\gamma V$ to $W\gamma$ cross section ratio grows very quickly and, for large values of $p_T(\gamma)$, exceeds the LO $W\gamma$ cross section. The effect is particularly pronounced in the $W^- \gamma$ case. Naively one would expect that the $W\gamma V$ cross section is suppressed by $\mathcal{O}(\alpha)$ with respect to the LO cross section, i.e. the cross section ratio should be of $\mathcal{O}(0.1)$ or less. However, the LO $W\gamma$ cross section itself is suppressed by the so-called “radiation zero” [63] which causes the $W\gamma V$ to $W\gamma$ cross section ratio to be much larger than expected. For large photon transverse momenta, the rate for $W^- \gamma$ production is about a factor of 4 smaller than that for $W^+ \gamma$ production. Since the $W\gamma V$ cross section is dominated by the $W^+ W^- \gamma$ channel, the $W\gamma V$ to $W\gamma$ cross section ratio is larger in the $W^- \gamma$ channel.

The contributions of the weak boson emission processes $pp \rightarrow W\gamma V$ to the $\mathcal{O}(\alpha^3)$ $W\gamma$ cross section have to be compared with those of the combined $\mathcal{O}(\alpha)$ one-loop weak and photonic radiative corrections [21]. The results are shown in Table II. Note that Ref. [21] uses slightly different cuts and parameters than I do. However, these effects should approximately cancel in the cross section ratio. The relative sizes of the one-loop weak and photonic radiative corrections for $W^+ \gamma$ and $W^- \gamma$ production are approximately equal. In $W^+ \gamma$ production, δ (1-loop) and $\delta_{\text{incl}}(W^+ \gamma V)$ approximately cancel for the range of photon transverse momenta listed here. On the other hand, for $pp \rightarrow W^- \gamma$, a significant positive contribution remains when summing δ (1-loop) and $\delta_{\text{incl}}(W^- \gamma V)$.

As discussed above, experiments require one charged lepton in the selection of $W\gamma$ events. Leptonic V decays in

TABLE II. Relative size of the $W\gamma V$ contributions, $\delta(W\gamma V)$, and the combined $\mathcal{O}(\alpha)$ one-loop weak and photonic corrections, δ (1-loop), to $W\gamma$ production at the LHC as a function of the photon transverse momentum. Cross sections are normalized to the LO $W\gamma$ cross section. The results for the $\mathcal{O}(\alpha)$ one-loop weak and photonic radiative corrections are taken from Ref. [21]. Results are shown for inclusive V decays (δ_{incl}), and for the case where jets with $p_T(j) > 50$ GeV and $|\eta(j)| < 4.5$, and events with more than one charged lepton, are vetoed (δ_{veto}).

$p_T(\gamma)$	δ (1-loop) [21]	$\delta_{\text{incl}}(W^+ \gamma V)$	$\delta_{\text{incl}}(W^- \gamma V)$	$\delta_{\text{veto}}(W^+ \gamma V)$	$\delta_{\text{veto}}(W^- \gamma V)$
275 GeV	−8.0%	9.4%	16.3%	0.6%	0.8%
525 GeV	−17.0%	17.0%	33.8%	1.5%	2.1%
775 GeV	−23.4%	22.8%	56.5%	1.9%	2.7%

$W\gamma V$ production therefore have to be excluded, except for $Z \rightarrow \bar{\nu}\nu$. This will reduce δ_{incl} by about 20%–30%.

Because of the suppression of the LO $W\gamma$ cross section and the logarithmic growth of the $W\gamma j$ cross section with $p_T(\gamma)$ [see Eq. (7)], the NLO QCD corrections for $W\gamma$ production at the LHC are very large at high photon transverse momenta [42]. At large $p_T(\gamma)$, the NLO QCD $W\gamma$ cross section is dominated by the $qg \rightarrow W\gamma q'$ contribution, i.e. most $W\gamma$ events contain a hard jet. Since the NLO QCD corrections significantly reduce the sensitivity to anomalous $WW\gamma$ couplings, it is advantageous to impose a jet veto. This strongly reduces the $W\gamma V$ cross section. I illustrate the impact of a jet veto in Fig. 8 and Table II for the case where jets with $p_T(j) > 50$ GeV and $|\eta(j)| < 4.5$ are vetoed, and only one charged lepton in events is allowed. In addition, the charged lepton and photon are required to be isolated from any jets which pass the cuts by $\Delta R(X, j) > 0.4$ ($X = \ell, \gamma$). The jet veto suppresses the $W\gamma V$ cross section by a factor 20–40. About one-half of the remaining $W\gamma V$ rate originates from $WZ\gamma$ production with $Z \rightarrow \bar{\nu}\nu$. Table II shows that, if a jet veto is imposed, the contribution from weak boson emission processes to the $\mathcal{O}(\alpha^3)$ cross section is much smaller than that from one-loop weak and photonic radiative corrections.

The results presented here demonstrate that contributions to the $W\gamma$ cross section from weak boson emission may be as important as those from the $\mathcal{O}(\alpha)$ virtual weak corrections. However, they also show that the size of these contributions depends very strongly on the event selection criteria.

Since the NLO QCD $W\gamma$ cross section at high $p_T(\gamma)$ is dominated by the tree-level process $qg \rightarrow W\gamma q'$, it still depends considerably on the factorization and renormalization scales (see e.g. Ref. [48]). The uncertainty from higher order QCD corrections in this region is roughly of the size of the contribution of the weak boson emission processes, i.e. in the 10%–50% range. Imposing a jet veto greatly reduces the scale uncertainty. In this case, the full $\mathcal{O}(\alpha)$ electroweak corrections which include virtual corrections and weak boson emission effects, will be significantly larger than the QCD scale uncertainty, and at least as large as the combined PDF and experimental systematic uncertainties.

$Z\gamma$, $Z \rightarrow \ell^+\ell^-$ events are selected by requiring two isolated charged leptons with opposite electric charge, and a hard, isolated photon. In addition, events should not have any significant amount of missing transverse momentum. In the following calculation, I impose the lepton and photon cuts of Eqs. (18)–(20), except the \cancel{p}_T cut. Instead, the missing transverse momentum in $Z\gamma$ events has to satisfy Eq. (11). The photon p_T cut strongly suppresses contributions from radiative Z decays which I shall ignore in the following.

In contrast to $W\gamma$ production there is no radiation zero in $pp \rightarrow Z\gamma$. The cross section for $Z\gamma V$, $V \rightarrow$ all, production

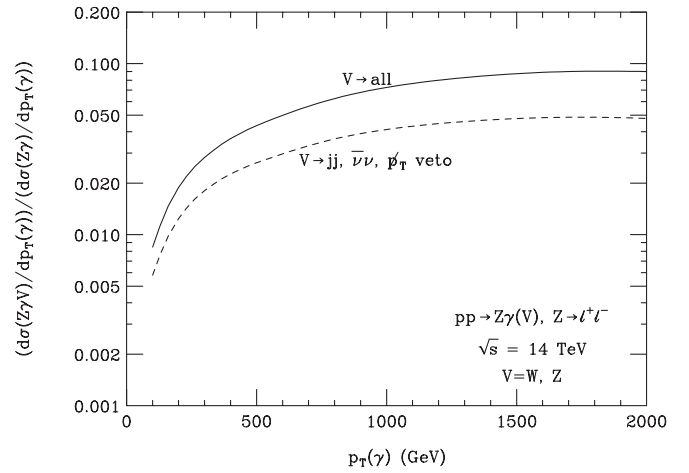


FIG. 9. Ratio of the $Z\gamma V$ ($V = W^\pm, Z$) and the LO $Z\gamma$ cross section as a function of the photon transverse momentum at the LHC. The Z boson is required to decay leptonically. Results are shown for the inclusive case, $V \rightarrow$ all (solid line), and for the case where events with more than two charged leptons and missing transverse momentum which does not satisfy Eq. (11) are vetoed (dashed line). The cuts imposed are listed in Eqs. (18)–(20).

(with no cuts imposed on the V decay products) therefore is 10% or less of the LO $Z\gamma$ rate over the entire photon transverse momentum range. This is shown by the solid line in Fig. 9. Since the LO $Z\gamma$ cross section is not suppressed, the NLO QCD corrections, especially at high $p_T(\gamma)$, are much smaller than for $W\gamma$ production, and there is no need to impose a jet veto when analyzing anomalous couplings [44]. Events with more than two charged leptons, however, are not included in a $Z\gamma$ sample. Vetoing events with more than two charged leptons, imposing the \cancel{p}_T veto of Eq. (11), and requiring that the photon and the charged leptons from $Z \rightarrow \ell^+\ell^-$ are isolated by

$$\Delta R(\ell, j) > 0.4, \quad \Delta R(\gamma, j) > 0.4 \quad (21)$$

from the jets which originate from V decays in $Z\gamma V$ production, one obtains the dashed line in Fig. 9. For $p_T(\gamma) = 300$ GeV (500 GeV), the $Z\gamma V$ cross section is approximately 1.9% (2.7%) of the LO $Z\gamma$ cross section. For comparison, the combined one-loop weak and photonic corrections, normalized to the LO $Z\gamma$ rate, are $-15 \pm 1\%$ ($-24 \pm 2\%$) at $p_T(\gamma) = 300$ GeV (500 GeV) [21]. Weak boson emission effects therefore only mildly affect the $Z\gamma$ production cross section.

The uncertainties from higher order QCD corrections in $Z\gamma$ production are similar to those for $W\gamma$ production when a jet veto is imposed. The full $\mathcal{O}(\alpha)$ electroweak corrections, including both virtual corrections and weak boson emission effects, will be at least as large as the combined theoretical and experimental systematic uncertainties. They cannot be neglected in a $Z\gamma$ analysis at the LHC.

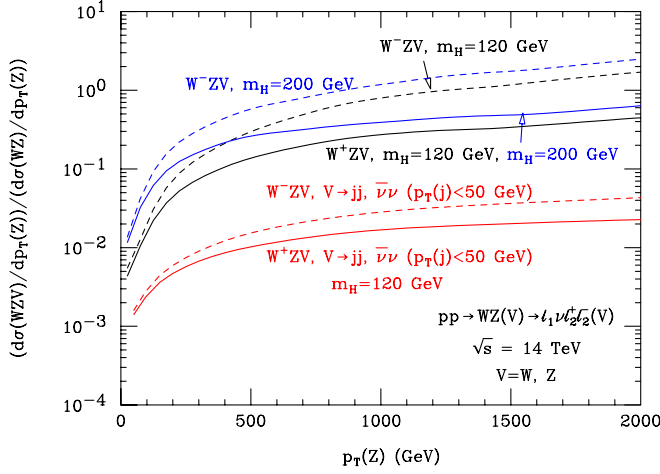


FIG. 10 (color online). Ratio of the WZV ($V = W^\pm, Z$) and the LO WZ cross section as a function of the Z transverse momentum at the LHC. Results are shown for the inclusive case, $V \rightarrow$ all (black and blue solid and dashed lines), and for the case where jets with $p_T(j) > 50$ GeV and $|\eta(j)| < 4.5$, and events with more than three charged leptons are vetoed (red solid and dashed lines). The black (blue) lines correspond to $m_H = 120$ GeV ($m_H = 200$ GeV). In the red curves, the Higgs boson mass is fixed to $m_H = 120$ GeV. The W and Z bosons are required to decay leptonically, $WZ \rightarrow \ell_1 \nu \ell_2^+ \ell_2^-$ ($\ell_{1,2} = e, \mu$). The cuts imposed are discussed in the text.

B. WZ and ZZ production

Weak boson emission effects in WZ and ZZ production are very similar to those in $pp \rightarrow W\gamma$ and $pp \rightarrow Z\gamma$, respectively. If one or both of the weak bosons decay hadronically, the signal process is swamped by QCD background. For $Z \rightarrow \bar{\nu}\nu$ and $W \rightarrow \ell\nu$, WZ production cannot be discriminated from single W production. To select WZ events one therefore requires three charged leptons and missing transverse momentum. In ZZ production, in order to reduce the background sufficiently, either both Z bosons have to decay into charged leptons, or one of them decays into neutrinos and the other into charged leptons. In the following, I concentrate on the 4 lepton final state in ZZ production. To identify WZ and ZZ events, I impose the cuts listed in Eq. (18). In addition, in WZ production, I require that the \cancel{p}_T cut of Eq. (20) is satisfied. In $pp \rightarrow ZZ$, events which do not satisfy Eq. (11) are rejected.

The LO WZ cross section is suppressed by an approximate radiation zero [64]. There is no suppression mechanism in ZZ production. It is therefore not surprising that the ratio of the WZV and WZ cross section rises quickly with $p_T(Z)$, and, for inclusive V decays, becomes $\mathcal{O}(1)$ in the TeV region. This is shown by the black and blue lines in Fig. 10. The transverse momentum distribution of the Z boson is of particular interest because of its sensitivity to anomalous WWZ couplings. For 100 fb^{-1} , WZ events with a Z -boson p_T up to about 500 GeV will be produced. The weak boson emission processes contributing to WZ and ZZ

production, $pp \rightarrow WZV$ and $pp \rightarrow ZZV$ involve Higgs exchange diagrams. The relative cross section thus depends on the Higgs boson mass, m_H . The black lines in Fig. 10 correspond to $m_H = 120$ GeV which is close to the lower limit established by LEP2 [65]. The blue curves show the results for $m_H = 200$ GeV, the current upper 95% CL limit from a fit to all electroweak data [66]. The cross sections for WZV and ZZV production vary significantly with m_H only for small values of $p_T(Z)$. At large transverse momenta, V bremsstrahlung diagrams dominate, and the cross section depends only slightly on the Higgs boson mass. Since the W^-Z cross section is significantly smaller than that for W^+Z production, and the WZV cross section is dominated by W^+W^-Z production, the cross section ratio is larger in the W^-Z case.

As in $W\gamma$ production, the NLO QCD corrections to $pp \rightarrow WZ$ become very large in the high $p_T(Z)$ region, and it is advantageous to impose a jet veto [48]. Requiring that there are no jets with $p_T(j) > 50$ GeV and $|\eta(j)| < 4.5$ in the event reduces the WZV cross section to a few percent or less of the LO WZ rate. This is shown for $m_H = 120$ GeV by the red solid dashed lines in Fig. 10. In order not to overburden the figure, only results for $m_H = 120$ GeV are shown when a jet veto is imposed. The Higgs mass dependence with a jet veto imposed is similar to that encountered in the inclusive case.

The relative rate for weak boson emission in WZ production should be compared with that of the $\mathcal{O}(\alpha)$ virtual weak corrections. The combined one-loop weak and photonic corrections to WZ production were calculated in the high energy limit in Ref. [22] and listed as a function of the minimum transverse momentum of the Z boson, $p_T^{\min}(Z)$. These results are compared with the relative rate for weak boson emission in Table III. The relative rate Δ shown in the table is defined by

$$\Delta(X) = \frac{\sigma^X(p_T(Z) > p_T^{\min}(Z))}{\sigma_{\text{LO}}^{WZ}(p_T(Z) > p_T^{\min}(Z))}. \quad (22)$$

Without a jet veto, weak boson emission effects are as large as or larger than the combined virtual weak and photonic corrections to WZ production. If a jet veto is imposed, they become small. The calculation of $\Delta(WZ, 1\text{-loop})$ [22] uses a slightly different rapidity cut on the leptons. Furthermore, in order to ensure the validity of the high energy approximation, a cut on the rapidity difference between the Z boson and the lepton from $W \rightarrow \ell\nu$ of $\Delta y(Z\ell) < 3$ was imposed. Δ_{incl} and Δ_{veto} were calculated with the lepton rapidity cut of Eq. (18) and without a $\Delta y(Z\ell)$ cut. The dependence of the cross section ratios Δ_{incl} and Δ_{veto} on these cuts should, however, be mild. Nevertheless, this should be kept in mind when comparing the numbers for $\Delta(WZ, 1\text{-loop})$, Δ_{incl} and Δ_{veto} in Table III.

In ZZ production, the LO cross section is not suppressed, and weak boson effects are of $\mathcal{O}(10\%)$ or less. This is shown in Fig. 11, where the ZZV cross section,

TABLE III. Relative size of the WZV contributions, $\Delta(WZV)$, and the combined $\mathcal{O}(\alpha^3)$ one-loop weak and photonic corrections, $\Delta(WZ, 1\text{-loop})$, to WZ production at the LHC as a function of the minimum Z boson transverse momentum, $p_T^{\min}(Z)$. Cross sections are normalized to the LO WZ cross section. The results for the combined $\mathcal{O}(\alpha^3)$ one-loop weak and photonic radiative corrections are taken from Ref. [22]. Results are shown for inclusive V decays (Δ_{incl}), and for the case where jets with $p_T(j) > 50$ GeV and $|\eta(j)| < 4.5$, and events with more than three charged lepton are vetoed (Δ_{veto}).

$p_T^{\min}(Z)$	250 GeV	300 GeV	400 GeV	500 GeV
$\Delta(WZ, 1\text{-loop})$ [22]	-10.9%	-13.1%	-17.8%	-21.2%
$\Delta_{\text{incl}}(W^+ZV), m_H = 120$ GeV	9.7%	11.1%	15.0%	17.7%
$\Delta_{\text{incl}}(W^-ZV), m_H = 120$ GeV	18.1%	21.7%	31.9%	41.7%
$\Delta_{\text{veto}}(W^+ZV), m_H = 120$ GeV	0.8%	0.9%	1.1%	1.3%
$\Delta_{\text{veto}}(W^-ZV), m_H = 120$ GeV	1.1%	1.2%	1.5%	1.8%
$\Delta_{\text{incl}}(W^+ZV), m_H = 200$ GeV	18.7%	24.4%	29.4%	31.3%
$\Delta_{\text{incl}}(W^-ZV), m_H = 200$ GeV	35.8%	45.5%	65.1%	76.8%
$\Delta_{\text{veto}}(W^+ZV), m_H = 200$ GeV	1.5%	2.0%	2.1%	2.2%
$\Delta_{\text{veto}}(W^-ZV), m_H = 200$ GeV	2.1%	2.6%	3.0%	3.4%

normalized to the LO ZZ rate, is displayed as a function of $p_T(Z)$ for the $ZZ \rightarrow e^+e^-\mu^+\mu^-$ channel. The black and blue solid lines show results for $m_H = 120$ GeV and $m_H = 200$ GeV for the inclusive $V \rightarrow$ all case. The dashed line represents the cross section ratio when events with more than four charged leptons are rejected, charged leptons are required to be isolated, $\Delta R(\ell, j) > 0.4$, and the \cancel{p}_T veto of Eq. (11) is imposed. The combined virtual weak and photonic corrections to ZZ production in the high energy approximation increase from about -20% for $p_T(Z) = 300$ GeV to $\approx -50\%$ at $p_T(Z) = 900$ GeV [22]. As in the $Z\gamma$ case, weak boson emission effects in ZZ production

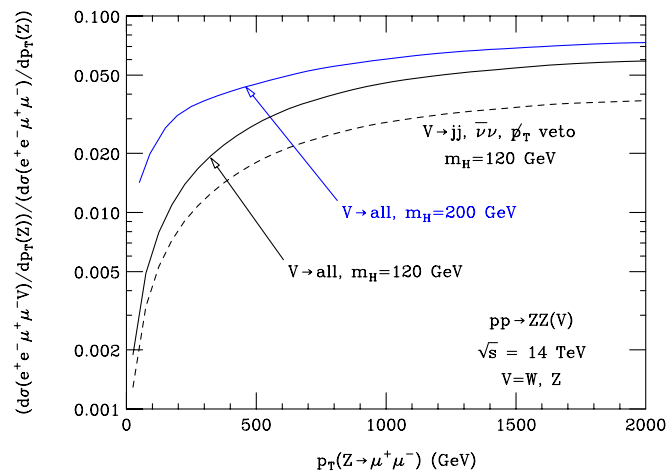


FIG. 11 (color online). Ratio of the ZZV and the LO ZZ cross section as a function of $p_T(Z \rightarrow \mu^+\mu^-)$ at the LHC. Only the $ZZ \rightarrow e^+e^-\mu^+\mu^-$ final state is considered. Results are shown for the inclusive case, $V \rightarrow$ all (black and blue solid lines), and for the case where events with leptonic decays of the third weak boson, V , are not allowed and a \cancel{p}_T veto is imposed (dashed line). The black (blue) lines correspond to $m_H = 120$ GeV ($m_H = 200$ GeV). The cuts imposed are discussed in the text.

are substantially smaller than the $\mathcal{O}(\alpha)$ virtual weak radiative corrections.

The uncertainties from higher order QCD corrections in WZ (ZZ) production are similar to those encountered in $W\gamma$ ($Z\gamma$) production. The $\mathcal{O}(\alpha)$ electroweak corrections to WZ and ZZ production, combining the virtual corrections in the high energy approximation and weak boson emission effects, will thus be significantly larger than the theoretical and experimental systematic uncertainties over most of the Z boson transverse momentum range.

C. WW production

W pair events are selected by requiring that both W bosons decay leptonically. In addition to two isolated charged leptons, a cut on the missing transverse momentum is imposed. In the calculations presented in this section, I impose the cuts of Eqs. (18) and (20) and concentrate on the $W^+W^- \rightarrow e^+\mu^-\cancel{p}_T$ final state. Since there is no radiation zero present in the $q\bar{q} \rightarrow W^+W^-$ helicity amplitudes, one would naively expect that the weak boson emission processes $pp \rightarrow WWV$ contributions are relatively small, as in the $Z\gamma$ and ZZ cases. However, this is only true in some kinematic distributions, such as the invariant mass distributions of the two leptons which is shown in Fig. 12. The WWV to LO WW cross section ratio as a function of the invariant mass of the two leptons is seen to be of $\mathcal{O}(1\%)$ or less once events with three or more leptons have been eliminated (red line). No restrictions on the jet activity, except for a $\Delta R(\ell, j) > 0.4$ cut, are imposed in results shown in Fig. 12. A jet veto, which is advantageous in suppressing the $t\bar{t}$ background [67], would considerably reduce the cross section ratio. The combined virtual weak and photonic $\mathcal{O}(\alpha)$ corrections to W -pair production in the high energy approximation reduce the LO WW cross section by 14% for $m(e^+\mu^-) \geq 500$ GeV and 23% for $m(e^+\mu^-) \geq 1$ TeV [22]. Weak boson emis-

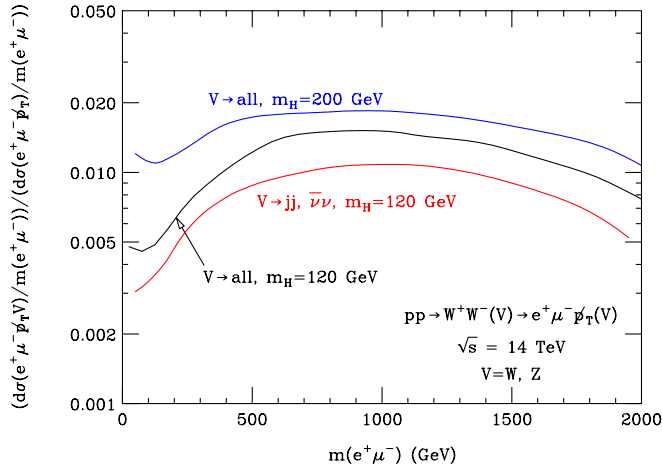


FIG. 12 (color online). Ratio of the WWV and the LO WW cross section as a function of the invariant mass of the two charged leptons, $m(e^+\mu^-)$, for the $W^+W^- \rightarrow e^+\mu^- \not{p}_T$ final state at the LHC. Results are shown for the inclusive case, $V \rightarrow$ all (black and blue lines), and for the case where events with leptonic decays of the third weak boson, V , are not allowed (red line). No restrictions on the jet activity in events are imposed. The black (blue) lines correspond to $m_H = 120$ GeV ($m_H = 200$ GeV). The cuts imposed are discussed in the text.

sion thus plays a minor role for the di-lepton invariant mass distribution in WW production.

The situation is completely different for the transverse momentum distribution of the di-lepton system, which is particularly sensitive to anomalous WWV couplings [68]. In the SM, the dominant W^\pm helicity at high energies in $\bar{u}u \rightarrow W^+W^-$ ($\bar{d}d \rightarrow W^+W^-$) is $\lambda_{W^\pm} = \mp 1$ ($\lambda_{W^\pm} = \pm 1$) [69–71] because of a t -channel pole factor which peaks at small scattering angles with an enhancement factor which is proportional to \hat{s} . Because of the $V-A$ nature of the $W\ell\nu$ coupling, the angular distribution of the charged lepton in the rest frame of the parent W is proportional to $(1 + Q_W \lambda_W \cos\theta)^2$, where Q_W is the W charge and θ is the angle with respect to the flight direction of the W in the parton center of mass frame. As a result, the charged leptons tend to be emitted either both into ($\bar{d}d$ annihilation), or both against the flight direction of their parent W boson ($\bar{u}u$ annihilation), i.e., they reflect the kinematic properties of the W bosons. At leading order, the W^+ and the W^- in W pair production are back to back in the transverse plane, and the transverse momenta of the two leptons tend to cancel at high energies. Above the W threshold, the SM $p_T(e^+\mu^-)$ distribution thus drops very rapidly.

The delicate balance of the lepton transverse momenta, however, is spoiled by real emission processes such as $pp \rightarrow WWV$. At large transverse momenta, weak boson emission therefore affects the $p_T(e^+\mu^-)$ differential cross section much more than other distributions. This is evident in Fig. 13 where I show the WWV to LO WW cross section ratio as a function of the di-lepton transverse momentum.

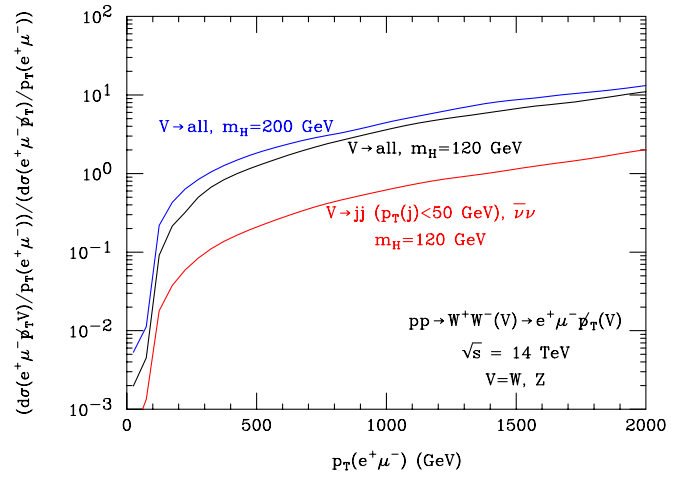


FIG. 13 (color online). Ratio of the WWV and the LO WW cross section as a function of the transverse momentum of the two charged leptons, $p_T(e^+\mu^-)$, for the $W^+W^- \rightarrow e^+\mu^- \not{p}_T$ final state at the LHC. Results are shown for the inclusive case, $V \rightarrow$ all (black and blue lines), and for the case where events with leptonic decays of the third weak boson, V , are not allowed and jets with $p_T(j) > 50$ GeV and $|\eta(j)| < 4.5$ are vetoed (red line). The black (blue) line corresponds to $m_H = 120$ GeV ($m_H = 200$ GeV). The Higgs boson mass is taken to be $m_H = 120$ GeV in the red line. The cuts imposed are discussed in the text.

In the inclusive case, $V \rightarrow$ all, the WWV rate exceeds the LO WW cross section for $p_T(e^+\mu^-) > 400$ GeV. The balance of the lepton transverse momenta is also upset by gluon radiation [68]. A jet veto helps reducing the size of the QCD corrections in the $p_T(e^+\mu^-)$ distribution. However, even when a jet veto is imposed, the WWV to LO WW cross section ratio still reaches about 15% at $p_T(e^+\mu^-) = 400$ GeV, the maximum di-lepton transverse momentum which can be probed at the LHC with an integrated luminosity of 300 fb^{-1} .

Reference [22] does not give results for how virtual weak and photonic radiative corrections in the high energy approximation affect the di-lepton transverse momentum distribution. Nevertheless, it is possible to make a qualitative statement about their size. At high energies, the virtual weak corrections are substantially larger than the photonic corrections. For $2 \rightarrow 2$ W pair production, the \not{p}_T and $p_T(e^+\mu^-)$ distributions are equal in absence of detector effects. In the high energy regime, the virtual weak corrections thus have a similar effect on the \not{p}_T and the di-lepton p_T distribution. For $\not{p}_T > 200$ GeV, the combined virtual weak and photonic $\mathcal{O}(\alpha)$ corrections reduce the WW cross section by about 20% [22]. It is therefore expected that the virtual weak corrections and the weak boson emission effects are roughly of the same magnitude and partially cancel even when a jet veto is imposed. Without a jet veto, W and Z radiation dominates over the virtual weak corrections for $p_T(e^+\mu^-)$ larger than about 200 GeV.

In addition to the p_T distribution of the di-lepton system, the maximal transverse momentum distribution of the charged leptons and the rapidity difference of the charged leptons are very sensitive to anomalous couplings and are also subject to large virtual electroweak corrections [72]. These distributions are sensitive to correlations between the charged leptons and weak boson emission effects thus are expected to considerably affect them.

Uncertainties from higher order QCD corrections in WW production at the LHC are similar in size to those encountered for the other di-boson production processes. For the di-lepton invariant mass distribution, the combined $\mathcal{O}(\alpha)$ virtual weak corrections and weak boson emission effects thus will be as large or larger than the combined theoretical and experimental systematic uncertainties. Although weak boson emission significantly reduces the size of the $\mathcal{O}(\alpha)$ electroweak corrections in the di-lepton p_T distribution, they are still non-negligible when compared with the expected systematic uncertainties.

V. TOP QUARK PRODUCTION

In this section, I investigate weak boson emission in top quark production processes. I consider top pair production, t -channel single top production, and tW production. There are three different types of single top quark production which can be distinguished by the virtuality of the W boson exchanged. In s -channel single top production, $q\bar{q}' \rightarrow W^* \rightarrow t\bar{b}, \bar{t}b$, the squared four-momentum of the W is positive, $Q_W^2 > 0$. In t -channel single top production, the W is exchanged in the t -channel and $Q_W^2 < 0$. Finally, in tW production, the W is on-shell, $Q_W^2 = M_W^2$. Weak boson emission in s -channel single top production has been studied in Ref. [29]. $t\bar{b}W$ production receives a large contribution from $\mathcal{O}(\alpha_s^2)$ $\bar{t}t$ production and has been found to be one of the dominant background sources for s -channel single top production [73]. s -channel single top production therefore is not considered here.

The top quark mass used in all calculations here is $m_t = 173$ GeV. This value agrees, within errors, with the most recent world average [74]. b -tagging efficiencies are not included in any numerical results presented in this section. The $\mathcal{O}(\alpha)$ electroweak radiative corrections to $\bar{t}t$ production at the Tevatron have been found to be quite small [26]. For t -channel single top and tW production, they have only been calculated for the LHC [27,28]. In the following, I therefore concentrate on top quark production at the LHC.

A. $\bar{t}t$ production

Top quark pair production at hadron colliders is important for several reasons. The top quark mass is a fundamental parameter of the SM and therefore should be measured as precisely as possible [74]. Measuring the $\bar{t}t$ cross section provides a test of the top quark production mechanism [75]. At the LHC, $pp \rightarrow \bar{t}t$ is also an important background to Higgs boson production [76].

In the following, I only consider the $\ell\nu b\bar{b} + \text{jets}$ final state; i.e. one top quark is required to decay semileptonically, and the other hadronically. Both b -quarks in the final state are assumed to be tagged. The following cuts are imposed on the final state particles:

$$p_T(\ell) > 20 \text{ GeV}, \quad |\eta(\ell)| < 2.5, \quad (23)$$

$$p_T(j) > 30 \text{ GeV}, \quad |\eta(j)| < 2.5, \quad (24)$$

$$p_T(b) > 30 \text{ GeV}, \quad |y(b)| < 2.5, \quad (25)$$

$$\not{p}_T > 40 \text{ GeV}, \quad \Delta R(i, k) > 0.4, \quad (26)$$

with $i, k = \ell, b, j$ and $i \neq k$. The number of nontagged isolated jets in the event, $n(j)$, is required to be $n(j) \geq 2$; a jet veto, i.e. requiring $n(j) = 2$, usually is not imposed [37,77]. One combination of a tagged b -quark and two isolated jets has to be consistent with originating from a hadronically decaying top quark. Only one charged lepton is allowed in the event. These requirements suppress $\bar{t}tV$ production with $V = W \rightarrow \ell\nu$ and $V = Z \rightarrow \ell^+\ell^-$ and I will ignore these channels here. However, $pp \rightarrow \bar{t}tV$ with $V \rightarrow jj$ and $V = Z \rightarrow \bar{\nu}\nu$ have to be considered when calculating the contribution of weak boson emission processes to top pair production. Finally, in order to suppress $\bar{t}tW$ production with $\bar{t}t \rightarrow \bar{b}b + 4$ jets and $W \rightarrow \ell\nu$, I require

$$\chi_{\min}^2 = \min_{b_1j_1j_2b_2j_3j_4\text{perm}} [\chi^2(b_1j_1j_2; b_2j_3j_4)] > 4, \quad (27)$$

where χ_{\min}^2 is the minimum of the $\chi^2(b_1j_1j_2; b_2j_3j_4)$ values of all possible combinations of jet pairs and bjj combinations, and

$$\begin{aligned} \chi^2(b_1j_1j_2; b_2j_3j_4) = & \frac{(m(j_1j_2) - M_W)^2}{\sigma_W^2} \\ & + \frac{(m(j_3j_4) - M_W)^2}{\sigma_W^2} \\ & + \frac{(m(b_1j_1j_2) - m_t)^2}{\sigma_t^2} \\ & + \frac{(m(b_2j_3j_4) - m_t)^2}{\sigma_t^2}. \end{aligned} \quad (28)$$

For the $W \rightarrow jj$ and $t \rightarrow bjj$ mass resolutions I assume $\sigma_W = 7.8$ GeV and $\sigma_t = 13.4$ GeV [77]. Only t and \bar{t} resonant diagrams are included in the calculation. Diagrams where the W or Z boson is emitted from one of the t or \bar{t} decay products are not taken into account.

The $\bar{t}tV$ to LO $\bar{t}t$ cross section ratio as a function of the transverse momentum of the t quark is shown in Fig. 14. The transverse momentum distributions for $\bar{t} \rightarrow \bar{b}\ell\nu$ and $\bar{t} \rightarrow \bar{b}jj$ are equal to those for semileptonic and hadronic t decays and therefore are not shown. For the cuts imposed, and with an integrated luminosity of 300 fb^{-1} , it should be

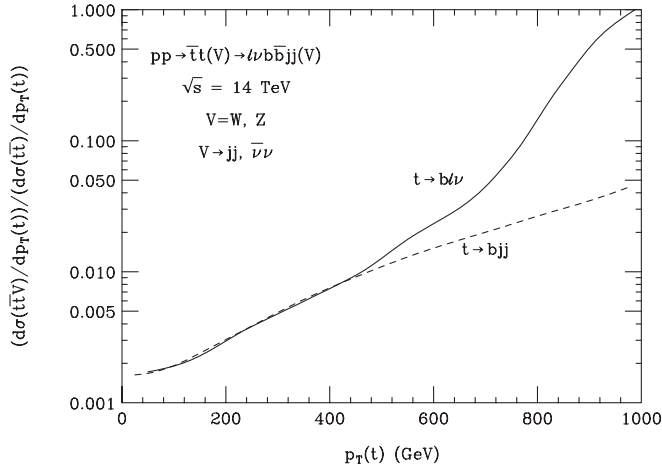


FIG. 14. Ratio of the $\bar{t}tV$ and the LO $\bar{t}t$ cross section as a function of the transverse momentum of the t quark. The solid (dashed) curve shows the result for $t \rightarrow b\ell\nu$ ($t \rightarrow bj\bar{j}$). The cuts imposed are discussed in the text.

possible to observe top quarks from $\bar{t}t$ production with a transverse momentum of up to 1 TeV at the LHC. Since gluon fusion does not contribute to $\bar{t}tW$ production, the inclusive $\bar{t}tV$ cross section is dominated by $pp \rightarrow \bar{t}tZ$. Below a transverse momentum of about 400 GeV, the cross section ratios for semileptonic ($t \rightarrow b\ell\nu$) and hadronic top decays ($t \rightarrow bj\bar{j}$) are essentially identical. For larger values of p_T , the cross section ratio for $t \rightarrow b\ell\nu$ grows significantly faster. The different behavior for semileptonic and hadronic top quark decays for $p_T(t) > 400$ GeV can be traced to the separation cut imposed on the final state particles [see Eq. (26)]. The separation cut is crucial for identifying $\bar{t}t \rightarrow \ell\nu b\bar{b}j\bar{j}$ events. For top quarks with very high transverse momenta, the decay products are highly boosted and thus almost collinear. This makes it increasingly difficult to satisfy Eq. (26). Since there is no separation cut imposed on the neutrino in $t \rightarrow b\ell\nu$, the ΔR cut is affecting the decay $t \rightarrow bj\bar{j}$ more significantly.

Because the separation cut suppresses hadronic t and \bar{t} decays at high transverse momentum, the top quark transverse momentum in $\bar{t}tV$ production is balanced by the p_T of the vector boson V for $t \rightarrow b\ell\nu$ and $p_T(t) > 500$ GeV. The transverse momentum of the hadronically decaying \bar{t} is typically small. On the other hand, in LO $pp \rightarrow \bar{t}t$, $p_T(t) = p_T(\bar{t})$. This implies that the growth of the $\bar{t}tV$ to LO $\bar{t}t$ cross section ratio at large $p_T(t)$ for semileptonic top decays is largely due to kinematic effects, and not a result of soft and/or collinear weak boson emission. The cross section ratio for $t \rightarrow b\ell\nu$ shown in Fig. 14 (solid line) therefore strongly depends on the ΔR cut imposed. For hadronic top decays, on the other hand, the milder increase of the cross section ratio is mostly due to the logarithmic enhancement factors associated with soft and/or collinear weak boson emission.

The $\mathcal{O}(\alpha)$ virtual weak corrections to $pp \rightarrow \bar{t}t$ for on-shell top quarks were calculated in Ref. [26]. For $p_T(t) =$

500 GeV ($p_T(t) = 1$ TeV) they reduce the LO $\bar{t}t$ cross section by about 5%–6% (10%–11%), depending on the Higgs boson mass. Since top quark decays and acceptance cuts equally affect the $\bar{t}t$ cross section with and without $\mathcal{O}(\alpha)$ virtual weak corrections, these values can be used as an estimate for how strongly the virtual weak corrections affect top quark pair production at the LHC. For $t \rightarrow bj\bar{j}$ and $p_T(t) = 500$ GeV ($p_T(t) = 1$ TeV), the $\bar{t}tV$ to $\bar{t}t$ cross section is about 1% (5%), and 1.5% (100%) for $t \rightarrow b\ell\nu$. If the top quark decays hadronically, weak boson emission effects thus partially compensate the effect of the $\mathcal{O}(\alpha)$ virtual weak corrections at high $p_T(t)$. On the other hand, for a semileptonically decaying top quark, weak boson emission effects dominate over the $\mathcal{O}(\alpha)$ virtual corrections for $p_T(t) > 800$ GeV. However, only very few events are produced in this region due to the separation cut [see Eq. (26)] imposed.

Since the growth of the $\bar{t}tV$ to LO $\bar{t}t$ cross section ratio in the $t \rightarrow b\ell\nu$ case is due to the kinematic cuts imposed, one expects a similar effect if the weak boson is replaced by a jet. In other words, the QCD corrections to top pair production at high $p_T(t)$ for $t \rightarrow b\ell\nu$ may be very large if a ΔR cut is imposed on the final state particles and $pp \rightarrow \bar{t}tj$ may well dominate the NLO QCD top pair cross section in this region. If this is the case, the factorization and renormalization scale uncertainty of the $\bar{t}t$ cross section in the high $p_T(t)$ region will be large, even when NLO QCD corrections are taken into account. Before one can determine whether it is important to take into account the $\mathcal{O}(\alpha)$ weak corrections, it will therefore be necessary to carefully investigate how NLO QCD corrections affect the $\bar{t}t$ cross section at high top quark transverse momentum in the presence of realistic acceptance cuts.

The discussion presented here has focused on the transverse momentum distribution of the top quark. Qualitatively similar results are found for the $\bar{t}t$ invariant mass distribution.

B. t -channel single top production

Single top production provides an opportunity to study the Wtb vertex [78]. To discriminate t -channel and s -channel single top production, one makes use of the final state produced and the event characteristics. In s -channel single top production, the top (or anti-top) quark is produced together with a high p_T b -quark. Additional jets produced via initial or final state radiation have a rapidity distribution peaked in the central region, $|\eta| < 2.5$. In t -channel single top production, on the other hand, the b -quark in the final state typically is soft, and the top quark is produced in association with a light quark jet. The rapidity distribution of the light quark jet peaks at $|\eta| \approx 3$. Jets originating from background processes such as $\bar{t}t$ or $Wj\bar{j}$ production, on the other hand, are predominantly produced with rapidity $|\eta| < 2.5$. To select t -channel single top production, I therefore require [37] one jet with

$$p_T(j) > 40 \text{ GeV}, \quad 2.5 < |\eta(j)| < 4.5, \quad (29)$$

and one b -jet (from top decay) with

$$p_T(b) > 35 \text{ GeV}, \quad |\eta(b)| < 2.5. \quad (30)$$

Additional b -jets with $p_T(b) > 35 \text{ GeV}$ and light quark or gluon jets with $p_T(j) > 40 \text{ GeV}$ are vetoed. The top quark is identified through its semileptonic decay, with the following cuts imposed on the charged lepton, $\ell = e, \mu$, and the missing transverse momentum:

$$p_T(\ell) > 20 \text{ GeV}, \quad |\eta(\ell)| < 2.5, \quad (31)$$

$$\cancel{p}_T > 40 \text{ GeV}. \quad (32)$$

I also assume that events do not contain a second charged lepton. Finally, a

$$\Delta R(i, k) > 0.4 \quad (33)$$

cut is imposed for $i, k = \ell, b, j$ and $i \neq k$. The cuts listed in Eqs. (29)–(33) are similar to those used in simulations by the CMS Collaboration [37]. Since events can only contain one b -jet, t -channel single top production can be calculated treating the initial state b -quark as a parton. Adopting this approach, at lowest order [$\mathcal{O}(\alpha^2)$], the process $pp \rightarrow tj$ and its charge conjugate, $pp \rightarrow \bar{t}\bar{j}$, contribute.

The weak boson emission processes relevant for t -channel single top production are $pp \rightarrow tjV$ and $pp \rightarrow \bar{t}\bar{j}V$ which I collectively denote as “ tjV production”. tjW production occurs at $\mathcal{O}(\alpha_s^2\alpha)$. The cross section for the weak boson emission process thus is potentially as large as that of the LO process. However, the central jet veto, and the forward jet tagging requirement [see Eq. (29)], suppress the tjV cross section. Since events with more than one charged lepton are vetoed, tjV production with $V = W \rightarrow \ell\nu$ and $V = Z \rightarrow \ell^+\ell^-$ does not contribute. In order to suppress events where the W boson from $t \rightarrow Wb$ decays hadronically and the other W leptonically, a cut on the $b\ell\cancel{p}_T$ cluster transverse mass, which peaks sharply at m_t , can be imposed.

If the W or Z boson produced in association with the tj system decays hadronically, the jet satisfying Eq. (29) may originate from weak boson decay. This configuration can easily be taken into account in the Z case since the cross section for tjZ production is finite. The $\mathcal{O}(\alpha_s^2\alpha)$ tjW cross section, however, diverges for small jet transverse momenta, and a calculation of $pp \rightarrow tW$, $W \rightarrow jj$ including NLO QCD corrections is needed. The NLO QCD corrections for tW production with $W \rightarrow \ell\nu$ have been calculated in Ref. [79] (see also [80]) and were subsequently incorporated into MCFM. In order to estimate the NLO QCD tW , $W \rightarrow jj$ cross section, I calculate tW , $W \rightarrow \ell\nu$ production, including NLO QCD corrections, for the cuts specified in

Eqs. (29)–(33) using MCFM, and rescale the cross section to correct for the larger $W \rightarrow jj$ decay rate. This approximation, of course, ignores QCD corrections associated with the decay of the W boson.

The calculation of Ref. [79] also takes into account the contributions from $\bar{t}t$ production where one of the b -quarks is soft, and one of the light quark jets satisfies Eq. (29). Top pair production, where one of the b -quarks is misidentified as a regular jet should then also be included in the calculation. Assuming a probability of 40% that a b -quark is misidentified as a light quark or gluon jet, I find that this process dominates weak boson emission for $p_T(t) \leq 200 \text{ GeV}$. It drops very rapidly at higher transverse momenta. In the intermediate region, $p_T(t) = 200\text{--}400 \text{ GeV}$, $tW(j)$ and tjZ production with $Z \rightarrow \bar{\nu}\nu$ are the main contributors, and for larger transverse momenta $pp \rightarrow tjZ(\rightarrow \bar{\nu}\nu)$ dominates.

Since the jet is required to be in the forward rapidity region [see Eq. (29)], the p_T distribution of the top quark falls very quickly. Vetoing additional jets in the event forces tjV events with $V \rightarrow jj$ into a phase space region which is very similar to that of the LO tj process. The $p_T(t)$ distribution for $pp \rightarrow tjV$ with $V \rightarrow jj$ therefore also falls very steeply. However, there are no phase space restrictions on the neutrinos produced in $pp \rightarrow tjZ$ with $Z \rightarrow \bar{\nu}\nu$. This results in a much harder $p_T(t)$ distribution. As a result, tjZ production with $Z \rightarrow \bar{\nu}\nu$ is the dominating weak boson emission process at large top quark transverse momenta. The $p_T(t)$ distribution for $pp \rightarrow tjZ$, $Z \rightarrow \bar{\nu}\nu$, is also much harder than that of the LO $pp \rightarrow tj$ process. The tjV to LO tj cross section ratio, which is shown in Fig. 15, therefore rises sharply at large $p_T(t)$. The dip at $p_T(t) \approx 300 \text{ GeV}$ is caused by the rapidly falling cross section for $\bar{t}t$ production where the b -quark is misidentified as a light quark jet. For 100 fb^{-1} , top quark transverse momenta up to about 500 GeV should be accessible.

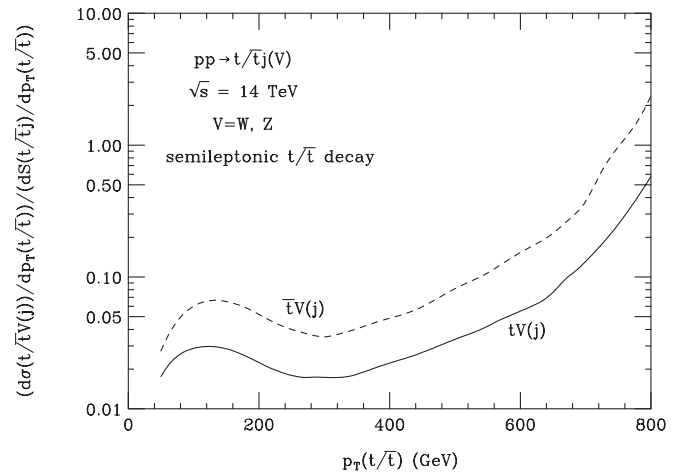


FIG. 15. Ratio of the $tV(j)$ ($\bar{t}V(j)$) and the LO tj ($\bar{t}\bar{j}$) cross section as a function of the transverse momentum of the t (\bar{t}) quark. The cuts imposed are discussed in the text.

At large top quark transverse momenta, one expects that gluon radiation frequently results in additional jets. The jet veto imposed suppresses these effects and results in Sudakov form factors which may have a significant impact on cross sections. However, the Sudakov form factors are expected to partially cancel in the tjV to tj cross section ratio.

The combined $\mathcal{O}(\alpha)$ virtual weak and photonic radiative corrections to tj production were presented in Ref. [27] as a function of the parton center of mass energy, $\sqrt{\hat{s}}$. For a top quark transverse momentum of $p_T(t) = 200$ GeV (400 GeV), the average parton center of mass energy is $\sqrt{\hat{s}} \approx 1$ TeV (1.7 TeV). The combined virtual weak and photonic $\mathcal{O}(\alpha)$ radiative corrections reduce the LO tj cross section by about 28% (36%) for $\sqrt{\hat{s}} = 1$ TeV (1.7 TeV). For comparison, the tjV ($\bar{t}jV$) cross section is about 2% (5%) of the LO tj ($\bar{t}j$) rate for both $p_T(t) = 200$ GeV and $p_T(t) = 400$ GeV. Weak boson emission thus has a relatively small effect on the electroweak radiative corrections in t -channel single top production at the LHC. Since the combined theoretical [81] and experimental [37] systematic uncertainties on the tj cross section are of $\mathcal{O}(10\%)$, it will be important to take the $\mathcal{O}(\alpha)$ virtual weak radiative corrections into account when analyzing t -channel single top production at the LHC.

C. tW production

The $pp \rightarrow tW$ process contains two W bosons and one b -quark in the final state. The W produced in association with the top quark has to decay leptonically in order to be identified. The top quark may decay semileptonically, $t \rightarrow \ell\nu b$ or hadronically, $t \rightarrow bj\bar{j}$. Both channels yield a signal of almost the same significance [37]. Since it allows for a straightforward reconstruction of the top quark transverse momentum, I only consider the $t \rightarrow bj\bar{j}$ final state here. Furthermore, since the cross sections for tW^- and $\bar{t}W^+$ production are equal, I focus on the process $pp \rightarrow tW^-$.

To compute the tW cross section, I impose the cuts listed in Eqs. (30)–(32) on the b -jet, the charged lepton and the missing transverse momentum. The non- b -like jets are required to have

$$p_T(j) > 35 \text{ GeV}, \quad |\eta(j)| < 2.5. \quad (34)$$

Lepton, b - and non- b -like jets are required to be isolated in $\eta - \phi$ space by

$$\Delta R(i, k) > 0.4 \quad (35)$$

($i, k = \ell, b, j, i \neq k$). The isolation cut strongly reduces the tW cross section at large top quark transverse momenta. Finally, the invariant mass of the $bj\bar{j}$ system has to be within 20 GeV of the top quark mass:

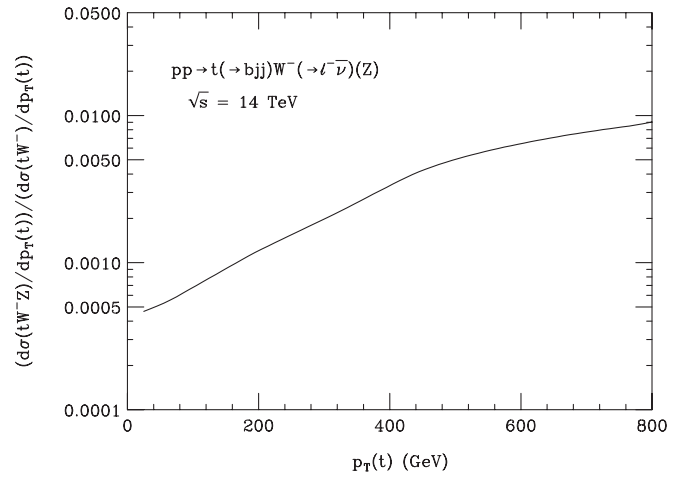


FIG. 16. Ratio of the tWZ and the LO tW cross section as a function of the transverse momentum of the top quark. The cuts imposed are discussed in the text.

$$|m(bj\bar{j}) - m_t| < 20 \text{ GeV}. \quad (36)$$

The dominant background to tW production arises from $pp \rightarrow \bar{t}t \rightarrow W^+W^-b\bar{b}$. To reduce the $\bar{t}t$ background, one tagged b -jet and two nontagged jets are required; events with additional b - or nontagged jets satisfying Eq. (34) are rejected. Likewise, events are not allowed to have a second charged lepton.

The only weak boson emission process for tW production is $pp \rightarrow tWZ$. Since hadronic Z decays are strongly suppressed by the jet veto and Eq. (36), it is not surprising that the ratio of the tWZ and LO tW cross sections, which is shown in Fig. 16 as a function of $p_T(t)$, is small. Although the fraction of tWZ events increases with $p_T(t)$, it is below 1% for top quark transverse momenta up to 800 GeV. For 100 fb^{-1} , top quarks with a transverse momentum of up to 600 GeV will be produced in the tW , $t \rightarrow bj\bar{j}$, $W \rightarrow \ell\nu$ channel with the cuts listed in Eqs. (34)–(36).

The combined $\mathcal{O}(\alpha)$ virtual weak and photonic radiative corrections to $pp \rightarrow tW$ were presented in Ref. [28] as a function of the parton center of mass energy, $\sqrt{\hat{s}}$. For a top quark transverse momentum of $p_T(t) = 200$ GeV, the average parton center of mass energy is $\sqrt{\hat{s}} \approx 700$ GeV for which the combined virtual weak and photonic $\mathcal{O}(\alpha)$ radiative corrections reduce the LO tW cross section by about 6%. For comparison, the tWZ cross section is about 0.13% of the LO tW rate for $p_T(t) = 200$ GeV. Weak boson emission thus is negligible in tW production. The electroweak $\mathcal{O}(\alpha)$ radiative corrections for $pp \rightarrow tW$ are substantially smaller than for t -channel single top production.

The combined theoretical [82] and experimental [37] systematic uncertainties of the tW cross section are about 15%–20%. They are considerably larger than the $\mathcal{O}(\alpha)$ electroweak radiative corrections.

VI. SUMMARY AND CONCLUSIONS

In the last five years, the $\mathcal{O}(\alpha)$ electroweak radiative corrections for a number of processes have been calculated. For some processes [5,11,13,83], higher order electroweak corrections were also calculated. At high energies, the virtual weak corrections become large and negative, due to soft and collinear logarithms of the form $(\alpha/\pi)\log^2(\hat{s}/M_{W,Z}^2)$. In QCD and QED, the corresponding terms diverge because gluons and photons are massless. The divergencies cancel when real gluon and photon emission is included in the calculation. Since the masses of the W and Z bosons act as infrared regulators, there is no technical reason for including weak boson emission in the calculation of weak radiative corrections. Furthermore, since W and Z bosons decay, weak boson emission leads to a different final state than the process considered. W and Z boson emission therefore is ignored in most calculations of electroweak radiative corrections.

However, this does not mean that these contributions may not be important at high energies, in particular, in inclusive processes. In this paper, I have investigated the importance of weak boson emission for those hadron collider processes for which the $\mathcal{O}(\alpha)$ virtual weak corrections are known to become large. In many cases, weak boson emission moderately reduces the effects of the $\mathcal{O}(\alpha)$ virtual weak corrections. Examples for processes where this is the case are inclusive jet, isolated photon, $Z + 1$ jet and Drell-Yan production. In some processes, such as $W\gamma$ and WZ production, weak boson emission may become large, unless a jet veto is imposed and the process becomes exclusive.

Conclusions about the size of weak boson emission effects may also depend on the observable considered. For example in charged Drell-Yan production, W and Z radiation is much more important in the lepton transverse momentum than in the transverse mass distribution. An even more extreme case are the p_T and invariant mass distributions of the charged lepton pair in $pp \rightarrow W^+W^- \rightarrow \ell_1^+\ell_2^-\not{p}_T$. In top pair production, the acceptance cuts may significantly affect the relative importance of the weak boson emission processes. Finally, in some processes

such as s -channel or t -channel single top production, the weak boson emission processes involve gluon exchange, although the LO process is purely weak. In this case, the cross section for the weak boson emission processes is potentially much larger than that of the LO process.

The calculations presented in this paper demonstrate that it is not possible to draw general conclusions about the importance of weak boson emission. The relevant processes have to be calculated in each case. This is straightforward and can be done efficiently using tools such as MADEVENT or AMEGIC++ [84]. General purpose Monte Carlo programs such as PYTHIA [85], or HERWIG [86] do not take into account weak boson emission.

The purpose of this paper has been to investigate for which processes and under what conditions weak boson emission may be important, not to add weak boson emission to existing calculations of the $\mathcal{O}(\alpha)$ virtual weak corrections. To do this, great care has to be taken to use the same definitions and input parameters for both the $\mathcal{O}(\alpha)$ virtual weak corrections, and weak boson emission. I have not done this; instead, for clarity, I opted for using one common set of input parameters [see Eqs. (1)–(3)]. Furthermore, in QCD related processes, I have taken into account QCD corrections to weak boson emission wherever possible. Ultimately, for the analysis of LHC data, a tool similar to MC@NLO [87] which contains the full $\mathcal{O}(\alpha)$ electroweak radiative corrections, including weak boson emission, for all relevant processes, together with an interface to a general purpose Monte Carlo program, is needed.

ACKNOWLEDGMENTS

I would like to thank E. Accomando, W. Bardeen, J. Campbell, Y. Gershtein, R. Harris, J. Huston, I. Iashvili, N. Kidonakis, S. Mrenna, S. Pozzorini, P. Skands, D. Wackerroth and M. Wobisch for useful discussions. I also would like to thank the Fermilab Theory Group, where part of this work was carried out, for its generous hospitality. This research was supported by the National Science Foundation under Grant No. PHY-0456681.

-
- [1] P. Ciafaloni and D. Comelli, Phys. Lett. B **446**, 278 (1999).
 - [2] M. Ciafaloni, P. Ciafaloni, and D. Comelli, Phys. Rev. Lett. **84**, 4810 (2000); Nucl. Phys. **B589**, 359 (2000).
 - [3] M. Ciafaloni, P. Ciafaloni, and D. Comelli, Phys. Lett. B **501**, 216 (2001).
 - [4] A. Denner and S. Pozzorini, Eur. Phys. J. C **18**, 461 (2001); **21**, 63 (2001).
 - [5] J.H. Kühn and A. A. Penin, hep-ph/9906545; J. H. Kühn,

- A. A. Penin, and V. A. Smirnov, Eur. Phys. J. C **17**, 97 (2000); J.H. Kühn, S. Moch, A. A. Penin, and V. A. Smirnov, Nucl. Phys. **B616**, 286 (2001); **B648**, 455(E) (2003); B. Jantzen, J.H. Kühn, A. A. Penin, and V. A. Smirnov, Phys. Rev. D **72**, 051301 (2005); **74**, 019901(E) (2006); Nucl. Phys. **B731**, 188 (2005); **B752**, 327(E) (2006).

- [6] For a review, see M. Melles, Phys. Rep. **375**, 219 (2003).

- [7] T. Kinoshita, *J. Math. Phys. (N.Y.)* **3**, 650 (1962); T. D. Lee and M. Nauenberg, *Phys. Rev.* **133**, B1549 (1964).
- [8] F. Bloch and A. Nordsieck, *Phys. Rev.* **52**, 54 (1937); V. V. Sudakov, *Sov. Phys. JETP* **3**, 65 (1956); D. R. Yennie, S. C. Frautschi, and H. Suura, *Ann. Phys. (N.Y.)* **13**, 379 (1961).
- [9] R. Doria, J. Frenkel, and J. C. Taylor, *Nucl. Phys.* **B168**, 93 (1980); G. T. Bodwin, S. J. Brodsky, and G. P. Lepage, *Phys. Rev. Lett.* **47**, 1799 (1981).
- [10] S. Moretti, M. R. Nolten, and D. A. Ross, *Phys. Rev. D* **74**, 097301 (2006); *Nucl. Phys.* **B759**, 50 (2006).
- [11] J. H. Kühn, A. Kulesza, S. Pozzorini, and M. Schulze, *J. High Energy Phys.* 03 (2006) 059.
- [12] E. Maina, S. Moretti, and D. A. Ross, *Phys. Lett. B* **593**, 143 (2004); **614**, 216(E) (2005).
- [13] J. H. Kühn, A. Kulesza, S. Pozzorini, and M. Schulze, *Phys. Lett. B* **609**, 277 (2005); *Nucl. Phys.* **B727**, 368 (2005).
- [14] U. Baur, O. Brein, W. Hollik, C. Schappacher, and D. Wackerroth, *Phys. Rev. D* **65**, 033007 (2002).
- [15] S. Dittmaier and M. Krämer, *Phys. Rev. D* **65**, 073007 (2002).
- [16] U. Baur and D. Wackerroth, *Phys. Rev. D* **70**, 073015 (2004).
- [17] A. Arbuzov, D. Bardin, S. Bondarenko, P. Christova, L. Kalinovskaya, G. Nanava, and R. Sadykov, *Eur. Phys. J. C* **46**, 407 (2006).
- [18] V. A. Zykunov, hep-ph/0509315; *Phys. At. Nucl.* **69**, 1522 (2006).
- [19] C. M. Carloni Calame, G. Montagna, O. Nicrosini, and A. Vicini, hep-ph/0609170.
- [20] E. Accomando, A. Denner, and S. Pozzorini, *Phys. Rev. D* **65**, 073003 (2002); W. Hollik and C. Meier, *Phys. Lett. B* **590**, 69 (2004).
- [21] E. Accomando, A. Denner, and C. Meier, *Eur. Phys. J. C* **47**, 125 (2006).
- [22] E. Accomando, A. Denner, and A. Kaiser, *Nucl. Phys.* **B706**, 325 (2005).
- [23] J. H. Kühn, A. Scharf, and P. Uwer, *Eur. Phys. J. C* **45**, 139 (2006); W. Bernreuther, M. Fückler, and Z. G. Si, *Phys. Lett. B* **633**, 54 (2006).
- [24] S. Moretti, M. R. Nolten, and D. A. Ross, *Phys. Lett. B* **639**, 513 (2006).
- [25] W. Beenakker, A. Denner, W. Hollik, R. Mertig, T. Sack, and D. Wackerroth, *Nucl. Phys.* **B411**, 343 (1994).
- [26] W. Bernreuther, M. Fückler, and Z. G. Si, hep-ph/0610334; J. H. Kühn, A. Scharf, and P. Uwer, hep-ph/0610335.
- [27] M. Beccaria, G. Macorini, F. M. Renard, and C. Verzegnassi, *Phys. Rev. D* **74**, 013008 (2006); hep-ph/0609189.
- [28] M. Beccaria, G. Macorini, F. M. Renard, and C. Verzegnassi, *Phys. Rev. D* **73**, 093001 (2006).
- [29] P. Ciafaloni and D. Comelli, *J. High Energy Phys.* 09, (2006) 055.
- [30] J. Pumplin, D. R. Stump, J. Huston, H. L. Lai, P. Nadolsky, and W. K. Tung, *J. High Energy Phys.* 07 (2002) 012.
- [31] M. L. Mangano, M. Moretti, F. Piccinini, R. Pittau, and A. D. Polosa, *J. High Energy Phys.* 07 (2003) 001.
- [32] A. Abulencia *et al.* (CDF II Collaboration), *Phys. Rev. Lett.* **96**, 122001 (2006); *Phys. Rev. D* **74**, 071103 (2006); CDF Report No. 8374 (2006); CDF Report No. 8388 (2006).
- [33] V. M. Abazov *et al.* (D0 Collaboration), D0 Report No. 5087 (2006).
- [34] U. Baur, E. W. N. Glover, and A. D. Martin, *Phys. Lett. B* **232**, 519 (1989).
- [35] Z. Kunszt and D. E. Soper, *Phys. Rev. D* **46**, 192 (1992); S. D. Ellis, Z. Kunszt, and D. E. Soper, *Phys. Rev. Lett.* **69**, 1496 (1992); **69**, 3615 (1992).
- [36] W. T. Giele, E. W. N. Glover, and D. A. Kosower, *Nucl. Phys.* **B403**, 633 (1993).
- [37] G. L. Bajatian *et al.* (CMS Collaboration), CERN Report No. CERN/LHCC 2006-021 (unpublished).
- [38] P. Aurenche, J. P. Guillet, E. Pilon, M. Werlen, and M. Fontannaz, *Phys. Rev. D* **73**, 094007 (2006).
- [39] D. Acosta *et al.* (CDF Collaboration), *Phys. Rev. D* **65**, 112003 (2002).
- [40] V. M. Abazov *et al.* (D0 Collaboration), *Phys. Lett. B* **639**, 151 (2006).
- [41] S. Frixione, P. Nason, and G. Ridolfi, *Nucl. Phys.* **B383**, 3 (1992).
- [42] U. Baur, T. Han, and J. Ohnemus, *Phys. Rev. D* **48**, 5140 (1993).
- [43] J. Ohnemus, *Phys. Rev. D* **51**, 1068 (1995).
- [44] U. Baur, T. Han, and J. Ohnemus, *Phys. Rev. D* **57**, 2823 (1998).
- [45] C. Roda, HCP2006, Duke University, 2006 (unpublished); V. Konopliankov, A. Ulyanov, and O. Kodolova, CMS Report No. 2006/042 (unpublished).
- [46] A. A. Affolder *et al.* (CDF Collaboration), *Phys. Rev. Lett.* **84**, 845 (2000).
- [47] B. Abbott *et al.* (D0 Collaboration), *Phys. Rev. Lett.* **84**, 2792 (2000); *Phys. Rev. D* **61**, 032004 (2000).
- [48] U. Baur, T. Han, and J. Ohnemus, *Phys. Rev. D* **51**, 3381 (1995).
- [49] J. M. Campbell and R. K. Ellis, *Phys. Rev. D* **60**, 113006 (1999).
- [50] J. M. Campbell and R. K. Ellis, <http://mcfm.fnal.gov>.
- [51] J. C. Pati and A. Salam, *Phys. Rev. Lett.* **31**, 661 (1973); *Phys. Rev. D* **10**, 275 (1974); R. N. Mohapatra and J. C. Pati, *Phys. Rev. D* **11**, 566 (1975); **11**, 2558 (1975); G. Senjanovic and R. N. Mohapatra, *Phys. Rev. D* **12**, 1502 (1975); J. L. Hewett and T. G. Rizzo, *Phys. Rep.* **183**, 193 (1989); E. Ma, *Phys. Rev. D* **36**, 274 (1987); K. S. Babu, X. G. He, and E. Ma, *Phys. Rev. D* **36**, 878 (1987); F. del Aguila, M. Quiros, and F. Zwirner, *Nucl. Phys.* **B287**, 419 (1987); M. Carena, A. Daleo, B. A. Dobrescu, and T. M. P. Tait, *Phys. Rev. D* **70**, 093009 (2004); T. Han, H. E. Logan, B. McElrath, and L. T. Wang, *Phys. Rev. D* **67**, 095004 (2003); N. Arkani-Hamed, A. G. Cohen, E. Katz, and A. E. Nelson, *J. High Energy Phys.* 07 (2002) 034.
- [52] L. Randall and R. Sundrum, *Phys. Rev. Lett.* **83**, 3370 (1999); **83**, 4690 (1999).
- [53] A. Abulencia *et al.* (CDF II Collaboration), CDF Report No. 7459 (2005); V. M. Abazov *et al.* (D0 Collaboration), D0 Report No. 5191-CONF (2006).
- [54] A. Abulencia *et al.* (CDF Collaboration), *Phys. Rev. Lett.* **96**, 211801 (2006); V. M. Abazov *et al.* (D0 Collaboration), D0 Report No. 4375-CONF (2004); D0 Report No. 4577-CONF (2004).
- [55] A. Abulencia *et al.* (CDF II Collaboration), CDF Report

- No. 8421 (2006) hep-ex/0611022; V. M. Abazov *et al.* (D0 Collaboration), Phys. Rev. Lett. **95**, 091801 (2005); D0 Report No. 5195-CONF (2006).
- [56] U. Baur, S. Keller, and W. K. Sakumoto, Phys. Rev. D **57**, 199 (1998).
- [57] F. Maltoni and T. Stelzer, J. High Energy Phys. 02 (2003) 027.
- [58] I. Belotelov *et al.*, CMS Report No. 2006/123 (2006).
- [59] J. Ellison and J. Wudka, Annu. Rev. Nucl. Part. Sci. **48**, 33 (1998).
- [60] V. Büscher and K. Jakobs, Int. J. Mod. Phys. A **20**, 2523 (2005).
- [61] J. Smith, D. Thomas, and W. L. van Neerven, Z. Phys. C **44**, 267 (1989); J. Ohnemus and J. F. Owens, Phys. Rev. D **43**, 3626 (1991); B. Mele, P. Nason, and G. Ridolfi, Nucl. Phys. **B357**, 409 (1991); J. Ohnemus, Phys. Rev. D **44**, 1403 (1991); **44**, 3477 (1991); **47**, 940 (1993); **50**, 1931 (1994); U. Baur, T. Han, and J. Ohnemus, Phys. Rev. D **53**, 1098 (1996); L. J. Dixon, Z. Kunszt, and A. Signer, Nucl. Phys. **B531**, 3 (1998); Phys. Rev. D **60**, 114037 (1999); D. De Florian and A. Signer, Eur. Phys. J. C **16**, 105 (2000); J. M. Campbell and R. K. Ellis, Phys. Rev. D **60**, 113006 (1999).
- [62] M. Dobbs and M. Levebvre, ATLAS Report No. ATL-PHYS-2002-023/ATL-PHYS-2002-022 (unpublished); S. Hassani, ATLAS Report No. ATL-PHYS-2003-022/ATL-PHYS-2003-023 (unpublished).
- [63] K. O. Mikaelian, Phys. Rev. D **17**, 750 (1978); K. O. Mikaelian, M. A. Samuel, and D. Sahdev, Phys. Rev. Lett. **43**, 746 (1979); R. W. Brown, K. O. Mikaelian, and D. Sahdev, Phys. Rev. D **20**, 1164 (1979); T. R. Grose and K. O. Mikaelian, Phys. Rev. D **23**, 123 (1981); S. J. Brodsky and R. W. Brown, Phys. Rev. Lett. **49**, 966 (1982); M. A. Samuel, Phys. Rev. D **27**, 2724 (1983); R. W. Brown, K. L. Kowalski, and S. J. Brodsky, Phys. Rev. D **28**, 624 (1983); R. W. Brown and K. L. Kowalski, Phys. Rev. D **29**, 2100 (1984).
- [64] U. Baur, T. Han, and J. Ohnemus, Phys. Rev. Lett. **72**, 3941 (1994).
- [65] R. Barate *et al.* (LEP Working Group for Higgs boson searches), Phys. Lett. B **565**, 61 (2003).
- [66] D. Wood, Proceeding at the XXXIII International Conference on High Energy Physics, Moscow, Russia, 2006.
- [67] D. Acosta *et al.* (CDF Collaboration), Phys. Rev. Lett. **94**, 211801 (2005).
- [68] U. Baur, T. Han, and J. Ohnemus, Phys. Rev. D **53**, 1098 (1996).
- [69] K. Hagiwara, R. D. Peccei, D. Zeppenfeld, and K. Hikasa, Nucl. Phys. **B282**, 253 (1987).
- [70] C. L. Bilchak and J. Stroughair, Z. Phys. C **23**, 377 (1984).
- [71] C. Bilchak, R. Brown, and J. Stroughair, Phys. Rev. D **29**, 375 (1984).
- [72] E. Accomando and A. Kaiser, Phys. Rev. D **73**, 093006 (2006).
- [73] T. Stelzer, Z. Sullivan, and S. Willenbrock, Phys. Rev. D **58**, 094021 (1998).
- [74] E. Brubaker *et al.* (The Tevatron Electroweak Working Group), hep-ex/0608032.
- [75] D. Glenzinski, The XXXIII International Conference on High Energy Physics, Moscow, Russia, 2006.
- [76] R. Kinnunen and D. Denegri, hep-ph/9907291.
- [77] M. Beneke *et al.*, hep-ph/0003033, and references therein.
- [78] S. Willenbrock and D. Dicus, Phys. Rev. D **34**, 155 (1986); C.-P. Yuan, Phys. Rev. D **41**, 42 (1990); R. K. Ellis and S. Parke, Phys. Rev. D **46**, 3785 (1992); D. Carlson and C.-P. Yuan, Phys. Lett. B **306**, 386 (1993); A. Heinson, A. Belyaev, and E. Boos, Phys. Rev. D **56**, 3114 (1997); S. Cortese and R. Petronzio, Phys. Lett. B **253**, 494 (1991); T. Stelzer and S. Willenbrock, Phys. Lett. B **357**, 125 (1995).
- [79] J. Campbell and F. Tramontano, Nucl. Phys. **B726**, 109 (2005).
- [80] S. Zhu, Phys. Lett. B **524**, 283 (2002); **537**, 351(E) (2002).
- [81] Z. Sullivan, Phys. Rev. D **70**, 114012 (2004).
- [82] N. Kidonakis, DPF2006, Honolulu, Hawaii, 2006.
- [83] A. Denner, B. Jantzen, and S. Pozzorini, Nucl. Phys. **B761**, 1 (2007).
- [84] F. Krauss, R. Kuhn, and G. Soff, J. High Energy Phys. 02 (2002) 044.
- [85] T. Sjostrand, S. Mrenna, and P. Skands, J. High Energy Phys. 05 (2006) 026.
- [86] G. Corcella *et al.*, hep-ph/0210213.
- [87] S. Frixione and B. R. Webber, hep-ph/0601192.